Supporting Information 1

Modulating β Arrestin-2 Recruitment at the δ- and μ-Opioid Receptors Using Peptidomimetic Ligands

Krishna K. Sharma,[1,†] Robert J. Cassell,[2,†] Yazan J. Meqbil,[2,7,†] Hongyu Su,[2] Arryn T. Blaine,[2,6] Benjamin R. Cummins,[3] Kendall L. Mores,[2] David K. Johnson,[8] Richard M. van Rijn,[2,4,5,‡] Ryan A. Altman[2,3‡]

[1]Division of Medicinal Chemistry and Pharmacognosy, College of Pharmacy, The Ohio State University, [2]Department of Medicinal Chemistry and Molecular Pharmacology, College of Pharmacy, Purdue University, [3]Department of Chemistry, Purdue University, [4]Purdue Institute for Drug Discovery, Purdue University, [5]Purdue Institute for Integrative Neuroscience, Purdue University, [6]Purdue Interdisciplinary Life Science Graduate Program, Purdue University, [7]Computational Interdisciplinary Graduate Program (CIGP), Purdue University, [8]Computational Chemical Biology Core and Molecular Graphics and Modeling Laboratory, The University of Kansas

[†]Contributed equally to this work

[‡]Corresponding Authors: Ryan A. Altman (raaltman@purdue.edu) and Richard M. van Rijn (rvanrijn@purdue.edu)

Table of Contents

General Synthetic Considerations

Unless specified, chemicals were purchased from commercial sources and used without further purification. Organic solvents used for synthesis were of analytical grade and used without further purification.

Proton nuclear magnetic resonance (^{1}H NMR) spectra, fluorine (^{19}F NMR), and carbon nuclear magnetic resonance (^{13}C NMR) spectra were recorded on a Bruker AVIII 500 AVANCE spectrometer with a BBFO cryoprobe (500, 376 and 126 MHz, respectively), a Bruker DRX 500 spectrometer with HR-mas probe (500, 376 and 126 MHz, respectively), Bruker AVIIIHD 400 MHz NMR with a broadband X-channel detect gradient probe (400, and 101 MHz, respectively), and Bruker AVIII 600 MHz NMR spectrometer equipped with a multi-nuclear broadband probe (600, 471 and 151 MHz, respectively). Chemical shifts (δ) for protons are reported in parts per million (ppm) downfield from tetramethylsilane, and are referenced to proton resonance of solvent residual peak in the NMR solvent (MeOD-d_4: δ = 4.87 ppm or DMSO-d_6: δ = 2.50 ppm). Chemical shifts (δ) for carbon atoms are reported in ppm downfield from tetramethylsilane, and are referenced to the carbon resonances of the solvent residual peak (MeOD-d_4: δ = 49.1 ppm or DMSO-d_6: δ = 39.52 ppm). Chemical shifts (δ) for fluorine atoms are reported in ppm relative to $PhCF_3$ (δ = −63.72 ppm). NMR data are represented as follows: chemical shift (ppm), multiplicity (s = singlet, d = doublet, dd = doublet of doublets, dt = doublet of triplets, dq = doublet of quartets, t = triplet, q = quartet, m = multiplet), coupling constant in Hertz (Hz), and integration. Exact mass analyses were furnished by using electrospray ionization using a time of flight mass analyzer (Waters LCT Premiere).

Peptidomimetics were synthesized using a Biotage Initiator microwave synthesizer using a solution-phase peptide synthesis protocol using Boc chemistry and 4N HCl in 1,4-dioxane for deprotection. Purification was conducted using a Teledyne ISCO EZ Prep system with a RediSep® C18 Prep column (30x250 mm, 100 Å, 5 μm spherical) using a gradient of 5% MeCN / 95% H_2O (with 0.1% acetic acid) to 95% MeCN/5% H_2O (with 0.1% acetic acid) over 45 min. The purity of final compounds was determined using a Hitachi instrument (L7000 series) equipped with a Vydac proteins and peptides C18 Column (3 μM, 4.6x250 mm), and using a gradient elution of MeCN and H_2O (0.1% TFA). The protocol for analytical HPLC was: flow rate = 1 mL/min, 0–4 min (5% MeCN/95% H_2O), 4–24 min (gradient 5 to 95% MeCN), 24–26 min (95% MeCN), 26–27 min (gradient 95 to 5% MeCN), 27–30 min (5% MeCN/95% H_2O).

Synthetic Chemistry

Synthesis of Boc-Tyr-ψ[(*Z*)CF=CH]-Gly-OH (7). Synthesis of Boc-Tyr-ψ[(*Z*)CF=CH]-Gly-OH (**7**) was carried out by previously developed and reported protocol from our laboratory.[1] All steps of this multistep synthetic sequence were repeated as reported, and all intermediates were characterized and found to be consistent with the reported literature.

Synthesis of 3b–d. Synthesis of N-α-Boc-Gly-Phe-Leu-OMe was achieved using Boc strategy of solution phase peptide synthesis under microwave irradiation with Leu-OMe.HCl (5 mmol) as starting material.[2] For synthesis of compounds **3b–d**, N-α-Boc-Gly-Phe-Leu-OMe (**2a**, 1 equiv., 2 mmol) was transferred to a round bottom flask, and the corresponding amine (NH_4OH, 5 mL or methylamine 40 wt% in H_2O, 5 mL or ethylamine solution 66–72% in H_2O, 5 mL) and methanol (1:1, 5 mL) were added to the flask at 0 °C. The reaction mixture was allowed to warm slowly to room temperature and was then stirred for 14 h. The reaction was monitored using TLC, and after consumption of starting material, the reaction mixture was concentrated under vacuum. The crude mixture was dissolved in a mixture of ethyl acetate and water, and then the layers were separated. The organic layer was concentrated under vacuum to afford desired compounds (**3b–d**). The synthesized peptides **3b–d** were characterized by NMR and mass spectrometry.

Synthesis of 3e–f. N-α-Boc-Gly-Phe-Leu-OH (**2**, 435 mg, 1 equiv., 1.4 mmol) was dissolved in DMF (1 mL) in a microwave (MW) reaction vessel. Amine (dimethylamine solution 2.0 M in THF, 1.4 mL, or cyclopropylamine, 195 µL, 2 equiv., 2.8 mmol), DIC (285 µL, 1.3 equiv., 2.8 mmol), and HONB (325 mg, 1.3 equiv., 2.8 mmol) were added to the reaction vessel, and the reaction mixture was heated under MW irradiation at 60 °C for 30 min.[2,3] Then, the crude peptides were dissolved in a mixture of ethyl acetate and water, and the layers were separated. The organic layer was concentrated under vacuum. The crude peptides were purified by RP-HPLC using a combination of acetonitrile and water (0.1% acetic acid) to afford compounds **3e–f**.

Synthesis of 3g. Compound **6** was purchased from a commercial source (Acros Organics, Fisher Scientific) and used in the synthesis of compound **3g**. Initially, **6** (300 mg, 1.2 equiv., 1.12 mmol) was dissolved in DMF (1 mL) in a microwave (MW) reaction vessel, and *N,N-d*iisopropylethylamine (DIEA, 523 µL, 3 equiv., 3.36 mmol) was added, and the solution was stirred to 5 min at room temperature. Next, *N*-α-Boc-Gly-Phe-OH (**2**, 300 mg, 1 equiv., 0.9 mmol), DIC (184 µL, 1.3 equiv., 1.17 mmol), and HONB (208 mg, 1.3 equiv., 1.17 mmol) were added to the reaction vessel, and the vial was sealed. The reaction mixture was heated under MW irradiation at 60 °C for 30 min to generate the crude *N*-α-Boc-Gly-Phe-*N*-phenyl-*N*-(piperidin-4-yl)propionamide (**3h**). Then, the crude peptide was dissolved in a mixture of ethyl acetate and water, and the layers were separated. The organic layer was concentrated under vacuum. The crude peptide was purified by RP-HPLC using a combination of acetonitrile and water (0.1% acetic acid) to afford pure compound **3h**, which was characterized by NMR and the mass spectroscopy.

General Procedure for Synthesis of Boc-Tyr-ψ[(*Z*)CF=CH]-Gly-Gly-Phe-Leu-X (1aa–ff). The synthesized compounds **3a−f** (0.2 mmol) were dissolved in a solution of 4N HCl in 1,4-dioxane (5 mL), and reaction mixtures

were stirred at room temperature for 30 min. The removal of 4N HCl in 1,4-dioxane under vacuum afforded the desired the Boc-deprotected peptidomimetics, and then, compounds were transferred to the MW vials for the coupling step. Next, deprotected compounds were neutralized with DIEA (3 equiv.) in DMF (1 mL) for 5 min at room temperature and then Boc-Tyr-ψ[(*Z*)CF=CH]-Gly-OH (**7**, 88 mg, 1.3 equiv., 0.26 mmol), DIC (40 μL, 1.3 equiv., 0.26 mmol), and HONB (46 mg, 1.3 equiv., 0.26 mmol) were added to the vial. The vial was sealed, and the reaction mixture was subjected to MW irradiated heating at 60 °C for 30 min at constant stirring. After completion of reaction, the crude peptidomimetics (**1aa–ff**) were dissolved in a mixture of ethyl acetate and water, and the layers were separated. The organic layer was concentrated under vacuum. The crude peptidomimetics (**1aa–ff**) were purified by RP-HPLC using a combination of acetonitrile and water (0.1% acetic acid) to afford pure compounds (**1aa–ff**), which was characterized by NMR and the mass spectroscopy.

General Procedure for Synthesis of H_2N-Tyr-ψ[(*Z*)CF=CH]-Gly-Gly-Phe-Leu-X (1a–f). Boc deprotection reactions were carried out under acidic conditions to afford the final compounds (**1a–f**). Compounds **1a–f** (0.15 mmol) were dissolved in a solution of 4N HCl in 1,4-dioxane (5 mL), and reaction mixtures were stirred at room temperature for 30 min. The removal of 4N HCl in 1,4-dioxane under vacuum afforded desired the Boc-deprotected peptidomimetics. The crude peptidomimetics (**1a–f**) were subjected to purification by RP-HPLC using a combination of acetonitrile and water (0.1% acetic acid) to afford pure compounds (**1a–f**), which were characterized by NMR and the high-resolution mass spectroscopy. The final purity of synthesized compounds was also analyzed using RP-UPLC and found to be ≥95%.

Synthesis of Boc-Tyr-ψ[(*Z*)CF=CH]-Gly-Gly-Phe-*N*-phenyl-*N*-(piperidin-4-yl)propionamide (1gg). The synthesized tripeptidomimetic **3g** (110 mg, 1 equiv., 0.2 mmol) was dissolved in a solution of 4N HCl in 1,4-dioxane (5 mL), and reaction mixture was stirred at room temperature for 30 min. 4N HCl in 1,4-dioxane was removed under vacuum and afforded desired the Boc-deprotected derivative, which was transferred to the MW vial for the coupling step. Next, the deprotected compound was dissolved in DMF (1 mL) and neutralized using DIEA (108 μL, 3 equiv., 0.6 mmol) for 5 min at room temperature. Then, Boc-Tyr-ψ[(*Z*)CF=CH]-Gly-OH (7, 88 mg, 1.3 equiv., 0.26 mmol), DIC (41 μL, 1.3 equiv., 0.26 mmol), and HONB (46 mg, 1.3 equiv., 0.26 mmol) were added, and the mixture was stirred well before subjecting to the microwave. The reaction mixture was subjected to MW irradiated heating at 60 °C for 30 min. After completion of reaction, the crude peptidomimetic **1gg** was dissolved in a mixture of ethyl acetate and water, and the layers were separated. The organic layer was concentrated under vacuum. The crude peptidomimetic **1gg** was purified by RP-HPLC using acetonitrile and water (0.1% acetic acid) solvent combination to afford pure compound, Boc-Tyr-ψ[(*Z*)CF=CH]-Gly-Gly-Phe-*N*-phenyl-*N*-(piperidin-4-yl)propionamide (**1gg**), which was characterized by NMR and the high-resolution mass spectroscopy.

Synthesis of H_2N-Tyr-ψ[(*Z*)CF=CH]-Gly-Gly-Phe-*N*-phenyl-*N*-(piperidin-4-yl)propionamide (1g). Deprotection of Boc-Tyr-ψ[(*Z*)CF=CH]-Gly-Gly-Phe-*N*-phenyl-*N*-(piperidin-4-yl)propionamide (**13g**) was carried out under acidic conditions to afford final peptidomimetic **1g**. Compound **1g** (33 mg, 0.04 mmol) was dissolved in a solution of 4N HCl in 1,4-dioxane (5 mL), and reaction mixture was stirred at room temperature for 30 min. The

removal of 4N HCl in 1,4-dioxane under vacuum afforded the desired the Boc-deprotected crude peptidomimetic **1h**. The crude product was subjected to purification by RP-HPLC using a combination of acetonitrile and water (0.1% acetic acid) to afford pure compound **1g**, which was characterized by NMR and the high-resolution mass spectroscopy. The final purity was analyzed using RP-UPLC and found to be ≥95%.

Spectroscopic Data

Boc-Gly-Phe-Leu-NH_2 (3b). Yield 85%, 1.38 g colorless solid. ^{1}H NMR (500 MHz, MeOD-d_4) δ 7.33–7.19 (m, 5H), 4.63 (m, 1H), 4.37 (m, 1H), 3.74–3.56 (m, 2H), 3.17 (m, 1H), 3.00 (dd, J = 16.1, 8.4 Hz, 1H), 1.68–1.59 (m, 3H), 1.45 (d, J = 4.2 Hz, 9H), 0.98–0.89 (m, 6H); ^{13}C NMR (126 MHz, MeOD-d_4) δ 175.8, 171.9, 171.4, 157.1, 136.7, 128.9, 128.2, 126.5, 79.4, 54.7, 51.6, 43.3, 41.3, 40.2, 36.9, 27.3, 24.3, 22.1; HRMS (ESI$^+$) mass calculated for $[M+H]^+$ ($C_{22}H_{35}N_4O_5$) m/z 435.2607, found m/z 435.2617.

Boc-Gly-Phe-Leu-NHMe (3c). Yield 84%, 335 mg colorless solid. ^{1}H NMR (400 MHz, MeOD-d_4) δ 7.34 (s, 1H), 7.23–7.06 (m, 6H), 4.50 (dd, J = 8.2, 5.6 Hz, 1H), 4.23 (m, 1H), 3.63–3.45 (m, 2H), 3.05 (dd, J = 13.9, 5.6 Hz, 1H), 2.86 (m, 1H), 2.58 (s, 3H), 1.58–1.42 (m, 3H), 1.32 (s, 9H), 0.86–0.75 (m, 6H); ^{13}C NMR (101 MHz, MeOD-d_4) δ 173.5, 171.9, 171.6, 157.1, 136.7, 128.9, 128.1, 126.5, 79.4, 54.8, 51.9, 43.3, 41.3, 40.2, 36.9, 27.2, 25.2, 24.3, 22.1, 22.1, 20.3; HRMS (ESI$^+$) mass calculated for $[M+H]^+$ ($C_{23}H_{36}N_4O_5$) m/z 449.2764, found m/z 449.2774.

Boc-Gly-Phe-Leu-NHEt (3d). Yield 96%, 407 mg colorless solid. ^{1}H NMR (400 MHz, $CDCl_3$) δ 7.29 (s, 1H), 7.21–7.13 (m, 4H), 7.08–7.05 (m, 2H), 7.01 (s, 1H), 5.42 (s, 1H), 4.71 (m, 1H), 4.45 (m, 1H), 3.85–3.67 (m, 2H), 3.27–3.10 (m, 3H), 3.02 (dd, J = 13.9, 6.0 Hz, 1H), 2.90 (dd, J = 13.8, 6.4 Hz, 1H), 1.62 (m, 1H), 1.45–1.28 (m, 11H), 1.07 (t, J = 7.3 Hz, 3H), 0.89–0.77 (m, 6H); ^{13}C NMR (101 MHz, $CDCl_3$) δ 171.5, 170.4, 169.4, 156.4, 136.0, 129.3, 128.6, 127.1, 80.4, 54.4, 51.9, 44.4, 41.1, 38.2, 34.4, 28.2, 24.6, 22.8, 14.6; HRMS (ESI$^+$) mass calculated for $[M+Na]^+$ ($C_{24}H_{38}N_4NaO_5$) m/z 485.2740, found m/z 485.2744.

Boc-Gly-Phe-Leu-NMe_2 (3e). Yield 60%, 390 mg colorless solid. ^{1}H NMR (400 MHz, MeOD-d_4) δ 8.00 (s, 1H), 7.33–7.14 (m, 5H), 4.69 (dd, J = 8.1, 5.5 Hz, 1H), 3.75–3.60 (m, 2H), 3.18–3.07 (m, 4H), 2.99–2.89 (m, 4H), 1.69–1.54 (m, 3H), 1.46 (s, 9H), 0.99–0.87 (m, 6H); ^{13}C NMR (101 MHz, MeOD-d_4) δ 173.9, 172.4, 170.7, 163.4, 136.7, 134.1, 129.0, 128.0, 126.3, 79.3, 54.0, 50.8, 44.2, 42.4, 36.1, 35.5, 34.7, 30.2, 27.3, 24.4, 22.1, 20.6; HRMS (ESI$^+$) mass calculated for $[M+H]^+$ ($C_{24}H_{39}N_4O_5$) m/z 463.2920, found m/z 463.2938.

Boc-Gly-Phe-*N*-phenyl-*N*-(piperidin-4-yl)propionamide (3g). Yield 42%, 210 mg colorless solid. ^{1}H NMR (500 MHz, MeOD-d_4) δ 7.67–7.38 (m, 3H), 7.32–7.11 (m, 5H), 7.11–6.92 (m, 2H), 5.06 (m, 1H), 4.72–4.58 (m, 1H), 4.50 (m, 1H), 3.87 (dd, J = 30.6, 13.8 Hz, 1H), 3.77–3.52 (m, 2H), 3.05 (m, 1H), 2.99–2.84 (m, 2H), 2.59 (m, 1H), 2.01–1.73 (m, 4H), 1.46 (s, 9H), 1.04–0.92 (m, 3H); ^{13}C NMR (126 MHz, MeOD-d_4) δ 174.4, 170.3, 169.8, 156.9, 138.1, 135.9, 129.9, 129.3, 129.1, 128.9, 128.5, 128.1, 128.0, 126.8, 79.3, 52.2, 49.7, 44.9, 43.0, 41.2, 38.4, 30.5, 29.6, 27.8, 27.2, 8.5. HRMS (ESI$^+$) mass calculated for $[M+Na]^+$ ($C_{30}H_{40}N_4NaO_5$) m/z 559.2896, found m/z 559.2906.

Boc-Tyr-ψ[(*Z*)CF=CH]-Gly-Phe-Leu-NH_2 (1bb). Yield 59%, 80 mg colorless solid. ^{1}H NMR (600 MHz, MeOD-d_4) δ 7.39–7.18 (m, 5H), 7.05 (d, *J* = 8.4 Hz, 2H), 6.72 (d, *J* = 8.0 Hz, 2H), 4.95 (m, 1H), 4.63 (m, 1H), 4.39 (m, 1H), 4.31 (m, 1H), 3.90–3.67 (m, 2H), 3.19 (dd, *J* = 14.0, 5.5 Hz, 1H), 3.10–2.86 (m, 4H), 2.74 (dd, *J* = 13.7, 8.7 Hz, 1H), 1.73–1.56 (m, 3H), 1.39 (s, 9H), 0.96 (d, *J* = 5.9 Hz, 3H), 0.93 (d, *J* = 5.9 Hz, 3H); ^{13}C NMR (151 MHz, MeOD-d_4) δ 177.4, 173.7, 173.4, 172.1, 161.3 (d, *J* = 260.6 Hz), 157.5, 157.1, 138.2, 131.4, 130.3, 129.6, 128.0, 116.2, 100.5 (d, *J* = 12.7 Hz), 80.4, 56.4, 54.8 (d, *J* = 28.9 Hz), 53.1, 49.9, 41.6, 38.4, 31.4 (d, *J* = 5.1 Hz), 28.7, 25.8, 23.6, 21.8; ^{19}F NMR (471 MHz, MeOD-d_4) δ -119.46 (dd, *J* = 36.3, 16.5 Hz); HRMS (ESI^+) mass calculated for $[M+H]^+$ ($C_{34}H_{47}FN_5O_7$) m/z 656.3460, found m/z 656.3480.

Boc-Tyr-ψ[(*Z*)CF=CH]-Gly-Phe-Leu-NHMe (1cc). Yield 62%, 265 mg colorless solid. ^{1}H NMR (500 MHz, MeOD-d_4) δ 7.34–7.20 (m, 5H), 7.05 (d, *J* = 8.5 Hz, 2H), 6.71 (d, *J* = 8.4 Hz, 2H), 4.95 (dt, *J* = 36.2, 7.5 Hz, 1H), 4.61 (m, 1H), 4.41–4.23 (m, 2H), 3.90–3.69 (m, 2H), 3.17 (dd, *J* = 14.0, 5.6 Hz, 1H), 3.08–2.94 (m, 3H), 2.91 (dd, *J* = 13.7, 6.4 Hz, 1H), 2.79–2.64 (m, 4H), 1.68–1.54 (m, 3H), 1.38 (s, 9H), 0.95 (d, *J* = 5.6 Hz, 3H), 0.90 (s, 3H); ^{13}C NMR (126 MHz, MeOD-d_4) δ 173.5, 172.3, 171.9, 170.6, 159.9 (d, *J* = 260.2 Hz), 156.1, 155.7, 136.7, 129.9, 128.9, 128.1, 128.1, 126.5, 114.7, 99.0 (d, *J* = 12.6 Hz), 79.0, 54.9, 53.3 (d, *J* = 29.1 Hz), 51.9, 42.4, 40.2, 36.9, 29.9 (d, *J* = 5.0 Hz), 27.3, 25.0, 24.3, 22.1, 20.4; ^{19}F NMR (471 MHz, MeOD-d_4) δ -119.38 (dd, *J* = 36.2, 16.0 Hz); HRMS (ESI^+) mass calculated for $[M+Na]^+$ ($C_{35}H_{48}FN_5NaO_7$) m/z 692.3435 , found m/z 692.3456.

Boc-Tyr-ψ[(*Z*)CF=CH]-Gly-Phe-Leu-NHEt (1dd). Yield 56%, 230 mg colorless solid. ^{1}H NMR (500 MHz, MeOD-d_4) δ 7.31–7.21 (m, 5H), 7.05 (d, *J* = 8.5 Hz, 2H), 6.71 (d, *J* = 8.5 Hz, 2H), 4.96 (m, 1H), 4.60 (dd, *J* = 8.5, 5.4 Hz, 1H), 4.39–4.25 (m, 2H), 3.88–3.66 (m, 2H), 3.26–3.12 (m, 3H), 3.05–2.86 (m, 4H), 2.73 (dd, *J* = 13.7, 8.6 Hz, 1H), 1.68–1.55 (m, 3H), 1.38 (s, 9H), 1.12 (t, *J* = 7.3 Hz, 3H), 0.95 (d, *J* = 5.9 Hz, 3H), 0.92 (d, *J* = 5.8 Hz, 3H); ^{13}C NMR (126 MHz, MeOD-d_4) δ 172.7, 172.3, 171.9, 170.6, 159.9 (d, *J* = 260.7 Hz), 156.1, 155.7, 136.7, 129.9, 128.9, 128.1, 128.1, 126.5, 114.7, 99.0 (d, *J* = 12.7 Hz), 79.0, 54.9, 53.3 (d, *J* = 28.6 Hz), 51.9, 42.5, 40.2, 36.9, 33.9, 30.0 (d, *J* = 5.2 Hz), 27.3, 24.4, 22.1, 20.4, 13.3; ^{19}F NMR (471 MHz, MeOD-d_4) δ -119.38 (dd, *J* = 36.2, 16.2 Hz); HRMS (ESI^+) mass calculated for $[M+H]^+$ ($C_{36}H_{51}FN_5O_7$) m/z 684.3773, found m/z 684.3793.

Boc-Tyr-ψ[(Z)CF=CH]-Gly-Phe-Leu-NMe_2 (1ee). Yield 44%, 98 mg colorless solid. ^{1}H NMR (500 MHz, MeOD-d_4) δ 7.31–7.18 (m, 5H), 7.05 (d, *J* = 8.5 Hz, 2H), 6.71 (d, *J* = 8.5 Hz, 2H), 4.95 (m, 1H), 4.69 (dd, *J* = 8.6, 5.4 Hz, 1H), 4.30 (m, 1H), 3.85–3.74 (m, 2H), 3.19–3.08 (m, 5H), 3.03 (d, *J* = 7.5 Hz, 2H), 2.97–2.87 (m, 5H), 2.73 (dd, *J* = 13.8, 8.6 Hz, 1H), 1.72–1.56 (m, 2H), 1.47 (ddd, *J* = 13.7, 9.1, 4.4 Hz, 1H), 1.38 (s, 9H), 0.98–0.93 (m, 6H); ^{13}C NMR (126 MHz, MeOD-d_4) δ 172.5, 172.1, 171.5, 169.8, 159.9 (d, *J* = 260.4 Hz), 156.1, 155.7, 136.7, 129.9, 128.9, 128.9, 128.0, 126.4, 114.7, 114.7, 99.0 (d, *J* = 12.7 Hz), 78.9, 54.2, 53.3 (d, *J* = 29.1 Hz), 42.1, 40.4, 37.4, 36.9, 36.1, 34.8, 30.1 (d, *J* = 5.2 Hz), 27.3, 24.4, 22.2, 20.6; ^{19}F NMR (471 MHz, DMSO-d_6) δ -116.7 (dd, *J* = 38.5, 14.5 Hz), -118.72 (dd, *J* = 30.4, 20.7 Hz); HRMS (ESI^+) mass calculated for $[M+H]^+$ ($C_{36}H_{51}FN_5O_7$) m/z 684.3773, found m/z 684.3772.

Boc-Tyr-ψ[(Z)CF=CH]-Gly-Phe-Leu-$NH^{Cy}Pr$ (1ff). Yield 56%, 120 mg colorless solid. ^{1}H NMR (600 MHz, MeOD-d_4) δ 7.34–7.28 (m, 2H), 7.28–7.22 (m, 3H), 7.06 (d, *J* = 8.6 Hz, 2H), 6.72 (d, *J* = 8.5 Hz, 2H), 4.95(m, 1H),

4.57 (dd, *J* = 8.6, 5.2 Hz, 1H), 4.35–4.26 (m, 2H), 3.85–3.67 (m, 2H), 3.18 (dd, *J* = 14.1, 5.2 Hz, 1H), 3.03 (d, *J* = 7.4 Hz, 2H), 3.01–2.88 (m, 2H), 2.76–2.64 (m, 2H), 1.73–1.52 (m, 3H), 1.39 (s, 9H), 0.97–0.90 (m, 6H), 0.77–0.68 (m, 2H), 0.59–0.48 (m, 2H); ^{13}C NMR (151 MHz, MeOD-d_4) δ 175.9, 173.7, 173.3, 172.2, 161.3 (d, *J* = 260.2 Hz), 157.6, 157.1, 138.1, 131.3, 130.3, 129.6, 129.5, 127.9, 116.1, 100.4 (d, *J* = 13.0 Hz), 80.4, 56.5, 54.8 (d, *J* = 28.9 Hz), 53.2, 49.8, 43.9, 41.5, 38.4, 38.2, 31.4 (d, *J* = 5.0 Hz), 28.7, 25.8, 23.5, 23.5, 21.8, 6.5, 6.4; ^{19}F NMR (471 MHz, MeOD-d_4) δ -119.4 (dd, *J* = 36.4, 16.3 Hz, 1F); HRMS (ESI$^+$) mass calculated for $[M+H]^+$ ($C_{37}H_{51}FN_5O_7$) m/z 696.3773, found m/z 696.3783.

Boc-Tyr-ψ[(Z)CF=CH]-Gly-Phe-*N*-phenyl-*N*-(piperidin-4-yl)propionamide (1gg). Yield 62%, 95 mg colorless solid. ^{1}H NMR (400 MHz, MeOD-d_4) δ 7.53–7.27 (m, 3H), 7.16 (m, 1H), 7.10–7.04 (m, 2H), 7.00–6.77 (m, 6H), 6.64–6.56 (m, 2H), 4.93 (dt, *J* = 12.0, 6.7 Hz, 1H), 4.55 (m, 1H), 4.42 (d, *J* = 13.6 Hz, 1H), 4.24 (m, 1H), 3.85–3.62 (m, 4H), 3.05–2.88 (m, 3H), 2.89–2.71 (m, 3H), 2.70–2.40 (m, 4H), 1.89–1.62 (m, 4H), 1.29 (s, 9H), 0.88 (td, *J* = 7.5, 5.5 Hz, 3H); ^{19}F NMR (376 MHz, MeOD-d_4) δ -118.90–-119.29 (m, 1F); HRMS (ESI$^+$) mass calculated for $[M+Na]^+$ ($C_{42}H_{52}FN_5NaO_7$) m/z 780.3748, found m/z 780.3768.

H_2N-Tyr-ψ[(Z)CF=CH]-Gly-Phe-Leu-NH_2 (1b). Yield 81%, 55 mg colorless solid. ^{1}H NMR (600 MHz, MeOD-d_4) δ 7.32–7.21 (m, 5H), 7.07 (d , *J* = 8.4 Hz, 2H), 6.76 (d, *J* = 8.5 Hz, 2H), 5.10 (m, 1H), 4.63 (dd, *J* = 8.7, 5.5 Hz, 1H), 4.38 (dd, *J* = 10.8, 3.6 Hz, 1H), 4.93 (m, 1H), 3.84 (d, *J* = 16.4 Hz, 1H), 3.73 (d, *J* = 16.4 Hz, 1H), 3.19 (dd, *J* = 14.0, 5.5 Hz, 1H), 3.12 (dd, *J* = 16.5, 7.9 Hz, 1H), 3.03–2.89 (m, 4H), 1.70–1.59 (m, 3H), 0.96 (d, *J* = 5.9 Hz, 3H), 0.92 (d, *J* = 5.8 Hz, 3H); ^{13}C NMR (151 MHz, MeOD-d_4) δ 177.3, 173.4, 173.1, 172.0, 157.8, 157.8 (d, *J* = 257.8 Hz), 138.2, 131.4, 130.3, 129.6, 127.9, 127.6, 116.5, 104.8 (d, *J* = 11.7 Hz), 56.4, 55.3 (d, *J* = 27.2 Hz), 53.0, 49.9, 43.8, 41.6, 38.4, 37.7, 31.2 (d, *J* = 4.5 Hz), 25.8, 23.6, 21.8; ^{19}F NMR (471 MHz, MeOD-d_4) δ -123.08 (dd, *J* = 36.6, 22.1 Hz, 1F); HRMS (ESI$^+$) mass calculated for $[M+H]^+$ ($C_{29}H_{39}FN_5O_5$) m/z 556.2930, found m/z 556.2949; purity ≥95%, rt 14.20 min.

H_2N-Tyr-ψ[(Z)CF=CH]-Gly-Phe-Leu-NHMe (1c). Yield 83%, 50 mg colorless solid. ^{1}H NMR (500 MHz, DMSO-d_6) δ 8.14–8.07 (m, 2H), 8.00 (d, *J* = 8.3 Hz, 1H), 7.57 (q, *J* = 4.6 Hz, 1H), 7.29–7.15 (m, 5H), 6.98 (d, *J* = 8.4 Hz, 2H), 6.66 (d, *J* = 8.5 Hz, 2H), 4.91 (dt, *J* = 38.8, 7.1 Hz, 1H), 4.49 (m, 1H), 4.22 (m, 1H), 3.72 (dd, *J* = 16.4, 5.7 Hz, 1H), 3.56 (dd, *J* = 16.4, 5.7 Hz, 1H), 3.45 (m, 1H), 3.02 (dd, *J* = 13.8, 4.5 Hz, 1H), 2.95–2.85 (m, 2H), 2.79 (dd, *J* = 13.8, 9.3 Hz, 1H), 2.72 (dd, *J* = 13.5, 5.9 Hz, 1H), 2.56 (s, 3H), 1.59–1.41 (m, 3H), 0.88 (d, *J* = 6.4 Hz, 3H), 0.83 (d, *J* = 6.4 Hz, 3H); ^{13}C NMR (126 MHz, DMSO-d_6) δ 172.5, 171.0, 170.5, 169.5, 162.5 (d, *J* = 257.8 Hz), 156.1, 138.1, 130.5, 129.6, 128.7, 128.5, 126.7, 115.4, 99.2 (d, *J* = 12.3 Hz), 54.5, 54.1 (d, *J* = 27.9 Hz), 51.5, 42.5, 41.2, 37.7, 30.4 (d, *J* = 4.6 Hz), 26.0, 24.6, 23.4, 22.0; ^{19}F NMR (470 MHz, DMSO-d_6) δ -121.02 (dd, *J* = 39.1, 15.7 Hz, 1F); HRMS (ESI$^+$) mass calculated for $[M+H]^+$ ($C_{30}H_{41}FN_5O_5$) m/z 570.3092, found m/z 570.3098; purity ≥95%, rt 14.52 min.

H_2N-Tyr-ψ[(Z)CF=CH]-Gly-Phe-Leu-NHEt (1d). Yield 62%, 79 mg colorless solid. ^{1}H NMR (500 MHz, MeOD-d_4) δ 7.32–7.19 (m, 5H), 7.06 (d, *J* = 8.4 Hz, 2H), 6.75 (d, *J* = 8.4 Hz, 2H), 4.99 (dt, *J* = 36.5, 7.4 Hz, 1H), 4.61 (dd, *J* = 8.5, 5.4 Hz, 1H), 4.34 (m, 1H), 3.88–3.69 (m, 3H), 3.26–3.03 (m, 4H), 3.03–2.84 (m, 4H), 1.68–1.54

(m, 3H), 1.12 (t, J = 7.3 Hz, 3H), 0.99–0.87 (m, 6H); ^{13}C NMR (126 MHz, MeOD-d_4) δ 172.7, 171.8, 171.8, 170.5, 157.9 (d, J = 259.5 Hz), 156.2, 136.7, 130.0, 128.9, 128.1, 126.6, 126.5, 115.1, 102.4 (d, J = 12.0 Hz), 54.9, 53.9 (d, J = 27.0 Hz), 51.8, 48.1, 47.9, 47.7, 47.6, 47.4, 47.2, 47.1, 42.3, 40.3, 37.0, 36.8, 33.9, 29.8 (d, J = 4.8 Hz), 24.4, 22.0, 20.5, 13.3; ^{19}F NMR (471 MHz, MeOD-d_4) δ -123.80 (dd, J = 34.8, 22.3 Hz, 1F); HRMS (ESI$^+$) mass calculated for $[M+H]^+$ ($C_{31}H_{43}FN_5O_5$) m/z 584.3248, found m/z 584.3268; purity ≥95%, rt 15.01 min.

H_2N-Tyr-ψ[(Z)CF=CH]-Gly-Phe-Leu-NMe_2 (1e). Yield 66%, 83 mg colorless solid. ^{1}H NMR (500 MHz, MeOD-d_4) δ 7.30–7.17 (m, 5H), 7.06 (d, J = 8.1 Hz, 2H), 6.75 (d, J = 8.0 Hz, 2H), 5.02 (dt, J = 36.5, 7.4 Hz, 1H), 4.69 (dd, J = 8.6, 5.3 Hz, 1H), 3.90–3.77 (m, 3H), 3.20–3.04 (m, 5H), 3.02–2.82 (m, 7H), 1.70–1.55 (m, 2H), 1.47 (ddd, J = 13.7, 9.0, 4.5 Hz, 1H), 0.96 (d, J = 6.5 Hz, 6H); ^{13}C NMR (126 MHz, MeOD-d_4) δ 174.0, 173.1, 173.0, 171.2, 159.4 (d, J = 259.1 Hz), 157.7, 138.2, 131.5, 130.4, 129.5, 128.1, 127.9, 116.6, 104.0 (d, J = 11.6 Hz), 55.7, 55.4 (d, J = 27.2 Hz), 43.5, 41.8, 38.9, 38.3, 37.6, 36.3, 31.4 (d, J = 4.9 Hz), 25.9, 23.6, 22.1; ^{19}F NMR (471 MHz, MeOD-d_4) δ -123.7 (dd, J = 33.9, 22.7 Hz, 1F); HRMS (ESI$^+$) mass calculated for $[M+H]^+$ ($C_{31}H_{43}FN_5O_5$) m/z 584.3252, found m/z 584.3256; purity ≥95%, rt 14.96 min.

H_2N-Tyr-ψ[(Z)CF=CH]-Gly-Phe-Leu-NH^{Cy}Pr (1f). Yield 85%, 80 mg colorless solid. ^{1}H NMR (600 MHz, MeOD-d_4) δ 7.38–7.14 (m, 5H), 7.07 (d, J = 8.2 Hz, 2H), 6.76 (d, J = 8.4 Hz, 2H), 5.09 (m, 1H), 4.59 (dd, J = 8.6, 5.2 Hz, 1H), 4.33 (dd, J = 10.0, 4.2 Hz, 1H), 3.95 (m, 1H), 3.85 (d, J = 16.4 Hz, 1H), 3.72 (d, J = 16.4 Hz, 1H), 3.23–3.05 (m, 2H), 3.05–2.91 (m, 4H), 2.66 (tt, J = 7.4, 3.9 Hz, 1H), 1.68–1.52 (m, 3H), 0.94 (d, J = 6.0 Hz, 3H), 0.91 (d, J = 5.8 Hz, 3H), 0.73 (dq, J = 6.3, 2.4 Hz, 2H), 0.60–0.49 (m, 2H); ^{13}C NMR (151 MHz, MeOD-d_4) δ 175.9, 173.3, 173.1, 172.1, 157.8 (d, J = 259.1 Hz), 157.8, 138.2, 131.5, 130.3, 129.6, 128.0, 127.6, 116.6, 105.0, 56.5, 55.3 (d, J = 27.2 Hz), 53.1, 43.9, 41.6, 38.4, 38.4, 37.6, 31.2 (d, J = 4.4 Hz), 25.9, 23.5, 23.5, 21.9, 6.5, 6.5; ^{19}F NMR (471 MHz, DMSO-d_6) δ -118.3 (dd, J = 39.1, 16.8 Hz, 1F); HRMS (ESI$^+$) mass calculated for $[M+H]^+$ ($C_{31}H_{43}FN_5O_5$) m/z 584.3253, found m/z 584.3257; purity ≥95%, rt 16.03 min.

H_2N-Tyr-ψ[(Z)CF=CH]-Gly-Phe-*N*-phenyl-*N*-(piperidin-4-yl)propionamide (1g). Yield 80%, 23 mg colorless solid. ^{1}H NMR (500 MHz, DMSO-d_6 at room temperature) δ 8.14 (t, J = 7.4 Hz, 1H), 7.95 (dt, J = 41.8, 6.0 Hz, 1H), 7.46 (dp, J = 40.0, 7.3 Hz, 3H), 7.24–7.08 (m, 4H), 7.06–6.89 (m, 5H), 6.67 (d, J = 8.0 Hz, 2H), 5.01–4.80 (m, 2H), 4.59 (dt, J = 24.2, 12.1 Hz, 1H), 4.36 (d, J = 13.2 Hz, 1H), 3.84 (dd, J = 36.5, 14.4 Hz, 3H), 3.02–2.66 (m, 7H), 2.53 (d, J = 15.7 Hz, 3H), 1.89–1.42 (m, 5H), 1.09–0.82 (m, 4H); ^{1}H NMR (500 MHz, DMSO-d_6 at 100 ºC) δ 7.73 (s, 1H), 7.62 (s, 1H), 7.45 (m, 1H), 7.23–6.92 (m, 9H), 6.69 (d, J = 8.1 Hz, 2H), 5.03–4.88 (m, 2H), 4.56 (m, 1H), 3.73–3.46 (m, 3H), 2.90 (dt, J = 20.7, 6.8 Hz, 4H), 2.77 (dd, J = 13.2, 6.8 Hz, 3H), 2.67–2.43 (m, 3H), 2.05–1.82 (m, 4H), 1.77–1.63 (m, 2H), 0.90 (d, J = 7.4 Hz, 3H); ^{13}C NMR (126 MHz, DMSO-d_6) δ 171.9, 169.8, 168.7, 168.5, 168.1, 162.2 (d, J = 258.4 Hz), 155.6, 138.5, 138.4, 137.2, 136.6, 130.2, 130.0, 129.3, 129.2, 128.9, 128.2, 128.0, 127.8, 126.4, 126.3, 114.9, 98.7 (d, J = 12.0 Hz), 53.7, 53.5, 51.5 (d, J = 15.5 Hz), 49.5, 49.0, 44.4, 44.1, 41.78, 41.7, 41.0, 40.8, 38.1, 37.6, 30.1, 29.9 (d, J = 15.5 Hz), 27.6, 9.4; ^{13}C NMR (126 MHz, DMSO-d_6 at 100 ºC) δ 171.7, 169.4, 168.4, 167.6, 162.4 (d, J = 259.3 Hz), 155.3, 138.5, 136.5, 129.7, 129.5, 128.8, 128.6, 128.0, 127.6, 127.5, 125.9, 114.7, 98.3–97.8 (m), 53.2 (d, J = 28.0 Hz), 51.8, 49.0, 41.8, 37.8, 29.6, 27.2, 8.8; ^{19}F NMR (471

MHz, DMSO-d_6 at room temperature) δ -118.1 (dd, J = 35.5, 18.7 Hz, 1F); ^{19}F NMR (471 MHz, DMSO-d_6 at 100 ºC) δ -117.1 (dd, J = 37.6, 15.1 Hz, 1F); HRMS (ESI$^+$) mass calculated for $[M+H]^+$ ($C_{37}H_{45}FN_5O_5$) m/z 658.3399, found m/z 658.3366; purity ≥95%, rt 16.03 min.

Pharmacological Characterization

Materials Used in the Cellular Signaling Assays. Leu-Enk and forskolin, were purchased from Sigma-Aldrich (St. Louis, MO USA). [D-Ala^2, N-MePhe^4, Gly-ol] enkephalin (DAMGO) was purchased from Tocris Bioscience (Minneapolis, MN, USA). Radiolabels were from Perkin Elmer (Waltham, MA, USA).

Cell Culture and Biased Signaling Assays. cAMP inhibition and β-Arr 2 recruitment assays were performed as previously described.[4] In brief, for cAMP inhibition assays HEK 293 (Life Technologies, Grand Island, NY, USA) cells were transiently transfected in a 1:3 ratio with FLAG-mouse δOR, or HA-mouse μOR and pGloSensor22F-cAMP plasmids (Promega, Madison, WI, USA) using Xtremegene9 (Sigma). Two days post-transfection cells (20,000 cells/well, 7.5 μl) were seeded in low volume Greiner 384-well plates (#82051-458, VWR, Batavia, IL, USA) and were incubated with GloSensor reagent (Promega, 7.5 μl, 2% final concentration) for 90 min at room temperature. Cells were stimulated with 5 μl drug solution for 20 min at room temperature prior to stimulation with 5 μl forskolin (final concentration 30 μM) for an additional 15 min at room temperature. For β-Arr recruitment assays, CHO-human μOR PathHunter β-Arr 2 cells or CHO-human δOR PathHunter β-Arr 2 cells (DiscoverX, Fremont, CA, USA) were plated (2,500 cells/well, 10 μl) one day prior to stimulation with 2.5 μl drug solution for 90 min at 37 °C/5% CO_2, after which cells were incubated with 6 μl cell PathHunter assay buffer (DiscoverX) for 60 min at room temperature as per the manufacturer's protocol. Luminescence for each of these assays was measured using a FlexStation3 plate reader (Molecular Devices, Sunnyvale, CA, USA).

Radioligand Binding Assay. For the binding assay 50 μl of a dilution series of peptide was added to 50 μl of 3.3 nM [^{3}H]DPDPE (K_d = 3.87 nM) or 2.35 nM of [^{3}H]DAMGO (K_d = 1.07 nM) in a clear 96 well plate. Next, 100 μl of membrane suspension containing 7 μg protein was added to the agonist wells and incubated for 90 min at room temperature. The reaction mixture was then filtered over a GF-B filter plate (Perkin Elmer) followed by 4 quick washes with ice-cold 50 mM Tris HCl. The plate was dried overnight, after which 50 μl scintillation fluid (Ultimagold uLLT) was added and radioactivity was counted on a Packard TopCount NXT scintillation counter. All working solutions were prepared in a radioligand assay buffer containing 50 mM Tris HCl, 10 mM $MgCl_2$, and 1 mM ethylenediaminetetraacetic acid at pH 7.4.

Calculation of Bias Factor. Bias factors were calculated using the operational model equation in Prism 8 to calculate Log R (τ/KA) (**Table S2**) as previously described.[4] Subsequently, bias factors were calculated using Leu-Enk as reference compound for δOR and μOR. Leu-Enk is more potent in the cAMP (G protein) assay than in the β-Arr 2 recruitment assay, and thus is not unbiased, but rather G protein-biased to begin with. A bias factor >1

meant that the agonist was more G protein-biased than the reference compound; A bias factor <1 meant that the agonist was less G protein-biased than the reference compound.

Data and Statistical Analysis. All data are presented as means ± standard error of the mean, and analysis was performed using GraphPad Prism 8 software (GraphPad Software, La Jolla, CA). For *in vitro* assays, nonlinear regression was conducted to determine pIC_{50} (cAMP) or pEC_{50} (β-Arr 2 recruitment). Technical replicates were used to ensure the reliability of single values, specifically each data point for binding and β-Arr recruitment was run in duplicate, and for the cAMP assay in triplicate. The averages of each independent run were counted as a single experiment and combined to provide a composite curve in favor of providing a 'representative' curve. In each experimental run, a positive control/reference compound was utilized to allow the data to be normalized and to calculate the log bias value. A minimum of three independent values were obtained for each compound in each of the cellular assays.

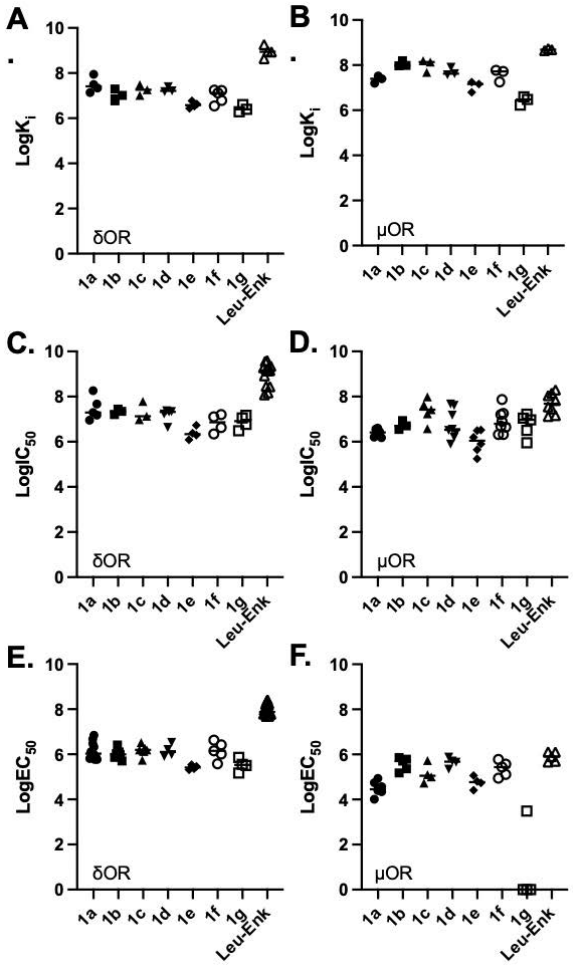

Chart SI-1. Raw Data for Binding Affinities, G Protein Coupling Activation, and β-Arrestin Recruitment at the μ and δ Opioid Receptors. (**A**) Binding Affinities at δOR; (**B**) Binding Affinities at μOR; (**C**) Inhibition of cAMP Production at δOR; (**D**) Inhibition of cAMP Production at μOR; (**E**) β-Arr 2 Recruitment at δOR; (**F**) β-Arr 2 Recruitment at μOR.

Solubility and Stability Studies

Assessment of Solubility. The solubility of **1e**,**f** and **1g** were measured in SGF and PBS using standard protocols. In brief, 100 mM stocks were prepared in DMSO, and 1/100 dilutions were performed to reach a 1 mM solution. After equilibration overnight on a roller mixer at rt (covered with foil), samples were filtered through 0.22 µm PVDF (aqueous) or 0.45 µm PTFE (organic) filters. The samples were then analyzed by LC-MS/MS and quantified against standards prepared in MeCN.

Assessment of Stability. Compounds **1e**,**f and 1g** were further characterized using standard physicochemical characterization and stability assays (Table SI-1) according to our previously published procedures.[5] Compounds **1e,f and 1g** were generally soluble in simulated gastric fluid (SGF) and PBS buffer (0.46–0.8 mM), though Pip-N(Ph)(COPh) analog **1g** displayed poor aqueous solubility (0.047–0.075 mM). This poor solubility of **1g** correlated with an increased logP value (2.09) relative to C-terminal amides **1e–f** (1.48–1.69). All analogs showed >1 mM solubility in 20% Captisol, and >0.78 mM in MeCN, MeOH, IPA. Overall, the analogs decomposed moderately in MeCN (ca. 30–50% decomposition at 48 h), though the compounds were generally stable in MeOH and IPA (ca. <5% decomposition at 48 h), which can be important for assay development. C-terminal NMe_2 (**1e**) showed excellent stability in simulated gastric fluid, PBS buffer, and SGF, PBS 20% captisol solution, though NHCyPr analog **1f** decomposed slowly in PBS and 20% Captisol (ca. 15–20% decomposition over 24 h). In contrast, Pip-N(Ph)(COPh) analog **1g** readily decomposed in SGF and PBS (ca. 40–90% decomposition over 48 h), indicating potential poor stability under biologically relevant conditions. Finally, stability of all compounds to mouse and human plasmas was assessed to study the influence of C-terminal modifications on *in vivo* plasma stability, which is the predominant route *in vivo* of metabolism and clearance,[6–8] for the endogenous enkephalins. C-terminal substituted analogs **1e**–**1f** were completely stable in mouse plasma, while Pip-N(Ph)(COPh) analog **1g** slowly degraded (25% degradation over 2 h) in human plasma.

Compound	**Solubility** (mM) SGF / PBS	**Solution Stability** ($\%T^0$ at 48 h) SGF / PBS / 20% Captisol	**Plasma Stability** ($\%T^0$ at 2 h) Mouse / Human
1a (OH)	0.19 / 0.20	>99% / 91% / 97%	>99% / >99%
1e (NMe_2)	0.60 / 0.45	95% / 92% / 93%	>99% / 88%
1f (NHCyPr)	0.61 / 0.45	>99% / 81% / 84%	>99% / >99%
1g [Pip-N(Ph)(COPr)]	0.075 / 0.047	59% / 11% / 100%	75% / >99%

Table SI-1. Experimental Solubility and Stability of Select Analogs.

The stabilities of analogs were monitored in mouse and human plasma (Innovative Research) at 37 °C. Compounds were spiked into plasma to obtain a concentration of 50 μM. At predetermined time points, samples were taken and quenched with acetonitrile, and the compounds were analyzed by LC-MS/MS. Samples were prepared in duplicate.

Calculated Bias Factors

Compound	δOR *Bias Factor*	δOR LogR cAMP	δOR LogR β-Arr 2	*μOR Bias Factor*	*μOR* LogR cAMP	*μOR* LogR β-Arr 2
1a (O^-)	1.2	7.17	6.15	0.4	6.14	4.35
1b (NH_2)	3.6	7.27	5.78	0.2	6.75	5.34
1c (NHMe)	1	6.96	6.02	0.9	7.13	5.15
1d (NHEt)	3.9	7.25	5.72	0.6	6.76	4.92
1e (NMe_2)	0.6	6.37	5.66	2.2	5.95	3.58
1f ($NH^{Cy}Pr$)	1.4	6.96	5.89	1.9	6.58	4.25
1g [Pip-N(Ph)(COEt)]	1.5	6.62	5.5	ND	6.02	nd
Leu^5-Enk	1	8.86	7.92	1	7.86	5.83

Table SI-2. Calculated Bias Factors.

Computational Methods

Protein and Peptide Preparation and System Setup

Crystal structures of the active δOR (6PT2)[9] bound to peptide agonist KGCM07 and μOR (5C1M)[10] bound to morphinan agonist BU7 were obtained from the Protein Data Bank (PDB). Structures were preprocessed to remove N-terminal tags, membrane lipids and other crystallized water molecules or ions not involved in mediating receptor-ligand interaction. The Protein Preparation Wizard[11,12] in the Schrödinger 2021-1 Suite (Schrödinger, Inc. NY, U.S.)[11] was used to prepare the structures for docking. A thermostabilizing mutation D108$^{(2.63)}$ in the peptide-bound δOR structure (6PT2)[9] was reversed to the wild-type (WT) residue K108 $^{(2.63)}$. Missing side chains and missing loops in the crystal structures were modeled using Prime.[11] The N-termini of the protein structures were capped. H-bond assignment was done using ProtAssign. The recently updated[12,13] OPLS4 forcefield[14–16] was used for energy minimization. Peptides were prepared using LigPrep, which generated the ionization states at pH 7.0 ± 2.0 using Epik.[17,18]Although they generated the cationic as well as the uncharged states, initial docking results strongly disfavored the uncharged state, so those were subsequently left out of the modeling studies.

Receptor Grid Generation and Peptide Docking using Glide[12-14]

Glide docking grids were generated from the prepared structures using the Receptor Grid Generational option in Glide using default parameters. The size of the enclosing box was enlarged to accommodate the bound ligand and allow for more peptide flexibility. The crystal ligands in both structures have a tyraminium substructure, while the crystallized δOR agonist peptide has a Phe in the 3 position and a di-CF_3 substituted benzene attached to the N-terminus of the 4-position sarcosine. On the other hand, the crystallized μOR ligand has even less in common with the peptide agonists **1a**–**g**. Peptides **1a**–**g** were first docked using Glide,[19–21] constraining the tyraminium substructures to the position found in the crystal structures, which allowed the N-terminal of each peptide to maintain its water-mediated interactions, as well as the salt bridge between the charged amine in the tyrosine derivative Dmt[1] and D128.

Peptides were initially docked using the standard precision (SP) scoring function, which treated the peptide as flexible, while rewarding intramolecular hydrogen bonds. Enhanced confirmational sampling was used, in which 50,000 poses per peptide were retained for the initial docking selection with a scoring window of 1000, while keeping the best 1,000 poses per ligand for energy minimization. The generated poses were rescored using the XP refining scoring function using the same parameters. In each case, 20 poses of each peptide were kept for post-docking energy minimization after which 10 poses were reported. Glide Emodel was used to rank the top 10 of poses of each peptide.

Peptides were then docked into the δOR structures using extended precision (XP) scoring function with a core constraint at the tyrosine side chain with the N-terminal nitrogen (which contains part of the tyraminium portion of the agonist), rewarding intramolecular hydrogen bonds, and a maximum of 10 poses per compound. This protocol samples potential interactions, while maintaining the well-established and conserved interactions involving the N-

termini of the peptides. The peptides with the C-terminal acid and NHMe had docked poses that scored very well compared to all the other peptides and shared the same interactions, particularly π-π stacking between Phe^{4} and W284$^{6.58}$.

Peptides were subsequently docked into μOR using Glide,[19–21] but with a different protocol, as the initial, lower-sampling protocol could not identify a pose that could explain the observed activities. Instead, the 12 compounds described by Cassell et al. that featured substitutions on the meta-position at the Phe^{4} of Leu^{5}-enkephalin,[22] were docked to μOR using extended (XP) precision, a core constraint of the tyraminium portion of the agonist, rewarding intramolecular hydrogen bonds, enhanced sampling, 50,000 poses per peptide in the first phase of docking, 1,000 scoring window for keeping initial poses, keeping the 1,000 best poses for in-docking energy minimizations, including aromatic H as donors, including 20 poses for post-docking minimization, and a maximum of 5 poses per compound. However, due to the absence of a larger common scaffold aside from the tyronnium substructure, in addition to the flexibility of the peptides, the reported poses share little resemblance to the agonist pose (Figures SI-1,3,5).

Top poses of the docked peptides at δOR and μOR were subsequently ranked using the SP-Peptide scoring function, which allows for more receptor flexibility. Peptides were treated as flexible, and aromatic hydrogens were included as donors while rewarding intramolecular hydrogen bonds. Default parameters for docking selection and pose minimization were used. The top 20 poses of each peptide were selected using a combination of Glide[12-14] docking scores, Glide Emodel and visual inspection (Figures SI-1,2,4). Refinements were made used Prime MMGBSA,[12,13,21] allowing for flexibility of any residue within 8 Å of the ligand. The docked energies and MMGBSA dG Bind energies are shown in Tables SI-3 and SI-4.

Molecular Dynamics Simulation of 1a (O^{-}) Docked into δOR.

The best selected pose of 1a (O^{-}) was used for a molecular dynamics (MD) simulation using Desmond in the Schrödinger suite 2021-1 (Figure SI-6).[23] Briefly, the peptide-protein complex was embedded in a POPC membrane contained in a TIP3P-solvated orthorhombic box while maintaining a 10 Å distance from box boundaries. The system was neutralized using chloride ions. Na^{+} and Cl^{-} ions at a concentration of 0.15M were added to mimic biological conditions using System Builder in Schrödinger 2021-1. The default relaxation protocol in Desmond was used to relax the membrane to a local energy minimum. RESPA integrator was used with a 2 fs integration step for bonded and short-range nonbonded forces and 6 fs for long-range nonbonded forces. Semi-isotropic coupling with the Nose-Hoover chain and Martyna-Tobias-Klein as the thermostat and barostat, respectively. Following the energy minimization simulation, a constant pressure (1.0 bar) and constant temperature (300.0K) NPT equilibration run was performed for the peptide-protein complex for 100 ns. For the production MD simulation, a 200 ns NPT simulation for the equilibrated protein-peptide complex were carried out.

Additional Computational Data and Figures

Table SI-3. Docking and MMGBSA dG Bind energy following refinement of modeled peptides against δOR.

Compound	**Docking Score** (kcal/mol)	**MMGBSA dG Bind** (kcal/mol)
1a (OH)	-8.487	-71.70
1b (NH_2)	-8.244	-75.40
1c (NHMe)	-8.314	-72.54
1d (NHEt)	-8.399	-79.63
1e (NMe_2)	-8.430	-82.58
1f (NHCyPr)	-7.191	-80.88
1g [Pip-N(Ph)(COEt)]	-7.368	-80.20

Table SI-4. Docking and MMGBSA dG Bind energy following refinement of modeled peptides against μOR.

Compound	**Docking Score** (kcal/mol)	**MMGBSA dG Bind** (kcal/mol)
1a (OH)	-8.675	-73.49
1b (NH_2)	-7.982	-67.32
1c (NHMe)	-8.209	-68.02
1d (NHEt)	-8.391	77.20
1e (NMe_2)	-4.931	-57.53
1f (NHCyPr)	-5.088	-65.45
1g [Pip-N(Ph)(COEt)]	-6.938	-75.96

Table SI-5. Phi and psi angles of modeled peptides against DOR, following refinement.

Compound	**Tyr[1]** Psi	**Gly[2]** Phi	Psi	**Gly[3]** Phi	Psi	**Phe[4]** Phi	Psi
1a (OH)	123.5	115.5	173.0	138.0	-174.3	-110.7	140.3
1b (NH_2)	138.2	84.9	179.1	138.1	-167.3	-118.7	155.5
1c (NHMe)	121.9	111.9	175.8	128.5	172.1	-85.3	106.1
1d (NHEt)	115.4	45.2	-140.2	125.2	--173.3	-73.6	59.8
1e (NMe_2)	115.5	47.3	-135.0	119.5	-175.3	-71.8	58.9
1f (NHCyPr)	126.5	66.9	-163.5	130.3	-177.5	-87.8	78.0
1g [Pip-N(Ph)(COEt)]	134.7	98.3	179.4	134.2	-167.5	-131.8	157.8

Table SI-6. Phi and psi angles of modeled peptides against μOR, following refinement.

Compound	**Tyr[1]** Psi	**Gly[2]** Phi	Psi	**Gly[3]** Phi	Psi	**Phe[4]** Phi	Psi
1a (OH)	92.5	-132.9	-1.8	-79.0	87.8	84.2	140.1
1b (NH_2)	-95.2	-122.1	1.4	-76.0	65.5	107.3	144.4
1c (NHMe)	85.0	-124.7	0.2	-76.5	77.4	90.0	137.8
1d (NHEt)	89.5	-134.4	-0.0	-83.1	95.4	78.8	165.4
1e (NMe_2)	105.1	56.2	-80.3	-78.4	112.3	74.3	152.4
1f (NHCyPr)	-122.4	-94.2	-26.5	-94.8	120.2	73.6	134.8
1g [Pip-N(Ph)(COEt)]	-132.1	67.0	-3.6	-75.0	-88.5	80.5	129.0

Because the peptide docking sampled low energy torsional space, the backbone phi and psi angles of Gly^3 and Phe^4 fell within acceptable Ramachandran space (Tables SI-5,6).

Table SI-7. Side chain dihedral angles of modeled peptides against DOR, following refinement.

Compound	**Tyr[1]** Chi1	Chi2	**Phe[4]** Chi1	Chi2	**Leu[5]** Chi1	**Phe[4]** Chi2
1a (OH)	173.2	-109.2	-62.1	140.5	-76.8	61.0
1b (NH_2)	-179.7	-114.1	-65.9	146.9	-78.1	60.4
1c (NHMe)	170.2	-108.3	-62.8	147.2	-72.3	64.9
1d (NHEt)	173.5	-135.8	-68.0	160.2	-84.7	65.2
1e (NMe_2)	174.4	-138.1	-68.1	160.5	-82.4	63.7
1f (NHCyPr)	174.9	-120.8	-68.4	154.4	-77.5	66.1
1g [Pip-N(Ph)(COEt)]	178.3	-110.4	-59.5	144.8	-53.9	46.3

Table SI-8. Side chain dihedral angles of modeled peptides against μOR, following refinement.

Compound	**Tyr[1]** Chi1	Chi2	**Phe[4]** Chi1	Chi2	**Leu[5]** Chi1	**Phe[4]** Chi2
1a (OH)	174.1	-151.2	-176.0	70.9	61.8	-77.3
1b (NH_2)	168.0	-142.0	-169.4	56.4	61.7	-77.1
1c (NHMe)	169.3	-144.8	-169.0	63.1	54.3	-85.0
1d (NHEt)	175.2	-157.3	-168.1	65.2	74.8	-64.5
1e (NMe_2)	176.9	-143	-172.8	68.4	72.0	-65.1
1f (NHCyPr)	-170.2	-174.5	-167.6	63.6	67.3	-79.1
1g [Pip-N(Ph)(COEt)]	176.4	-146.4	174.3	79.3	-53.6	45.7

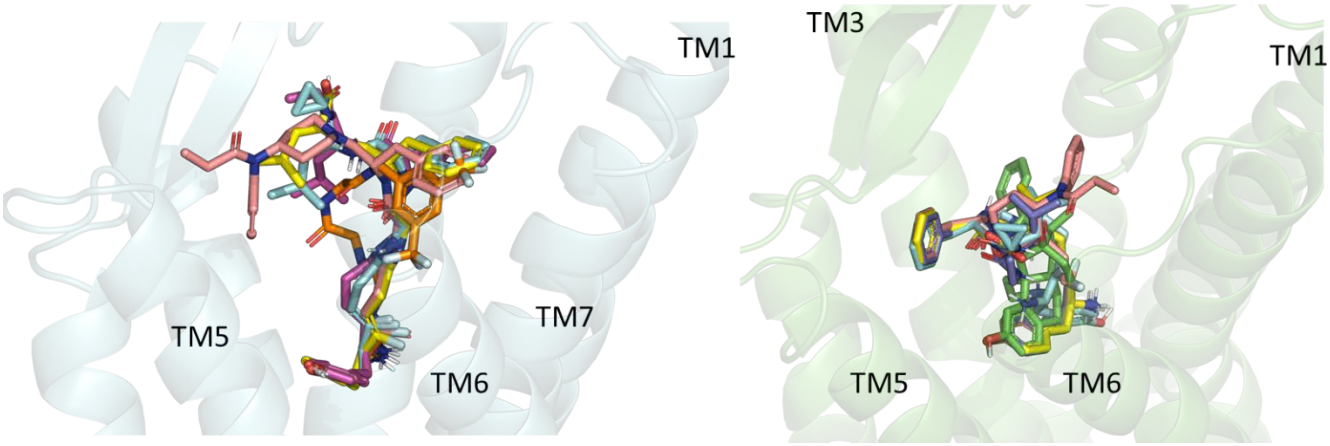

Figure SI-1: Peptide Models Superimposed with Crystal Ligands. Refined models of the peptides Leu-Enkephalin analogs bound to dOR (left, cyan) and μOR (right, green), superimposed with the crystal poses of KCGM07 and BU72, respectively. Crystal structures and known agonists were retrieved from PDB ID 6PT2 and PDB ID 5C1M. **1a** (O^-) yellow, **1d** (NHEt) purple, **1f** ($NH^{Cy}Pr$) cyan, **1g** [*N*-Pip-N(Ph)(COEt)], pink. δOR (cyan, PDB: 6PT2) and μOR (green, PDB: 5C1M).

1a

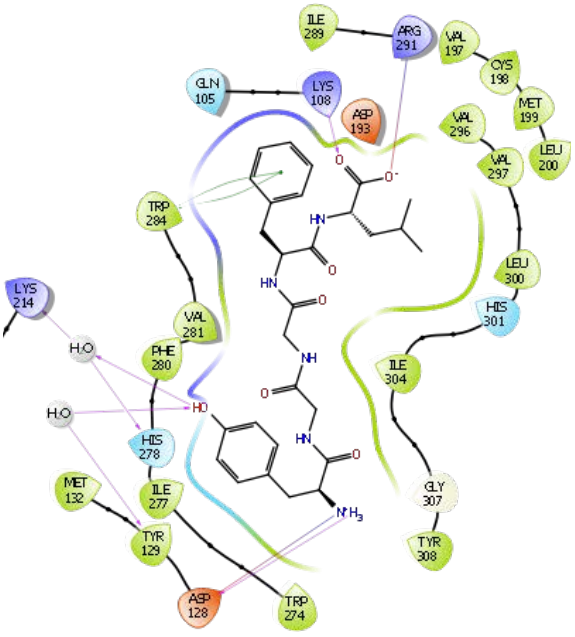

1b

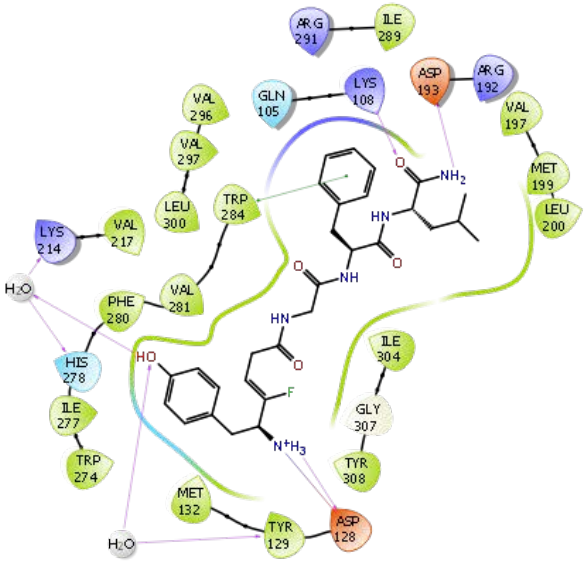

1c

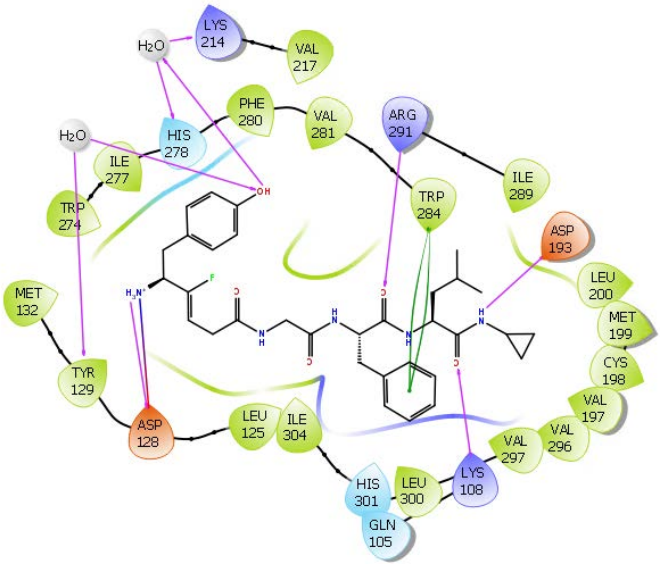
LYS 214
VAL 217
H2O
PHE 280
VAL 281
ARG 291
H2O
HIS 278
ILE 277
ILE 289
TRP 284
TRP 274
ASP 193
LEU 200
MET 132
MET 199
CYS 198
TYR 129
VAL 197
ASP 128
LEU 125
ILE 304
VAL 296
VAL 297
HIS 301
LEU 300
LYS 108
GLN 105

1d

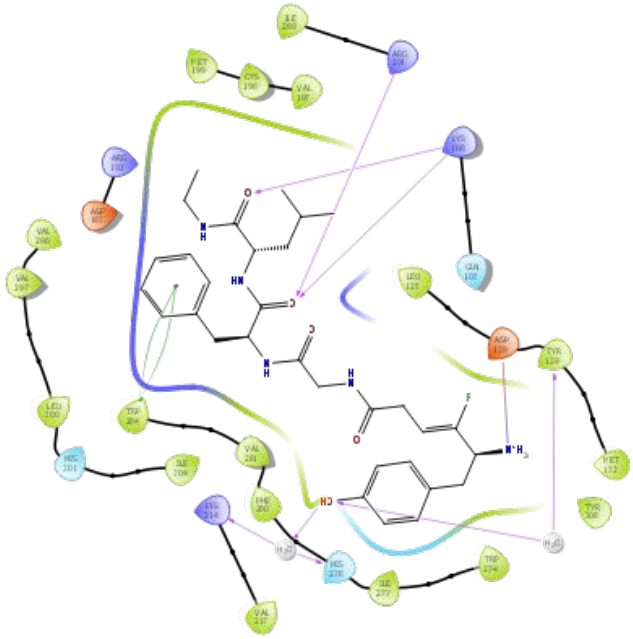

1e

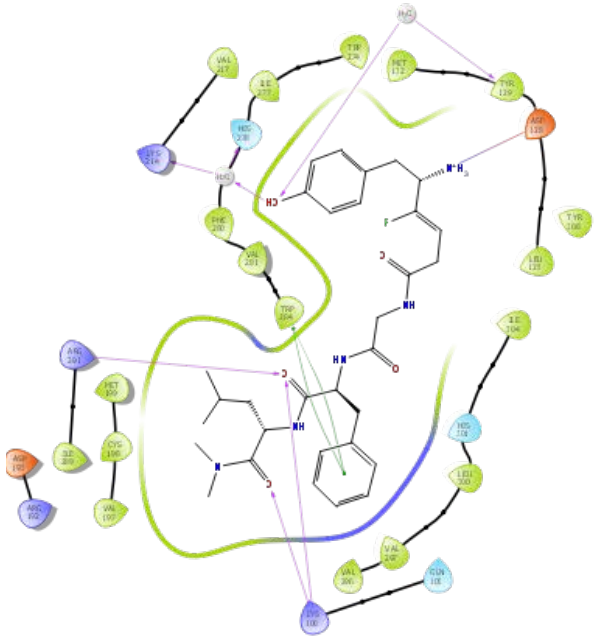

1f

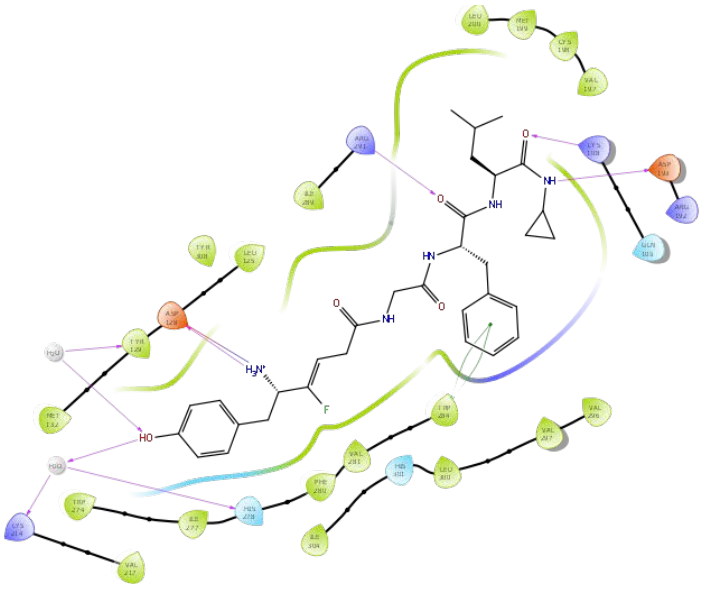

1g

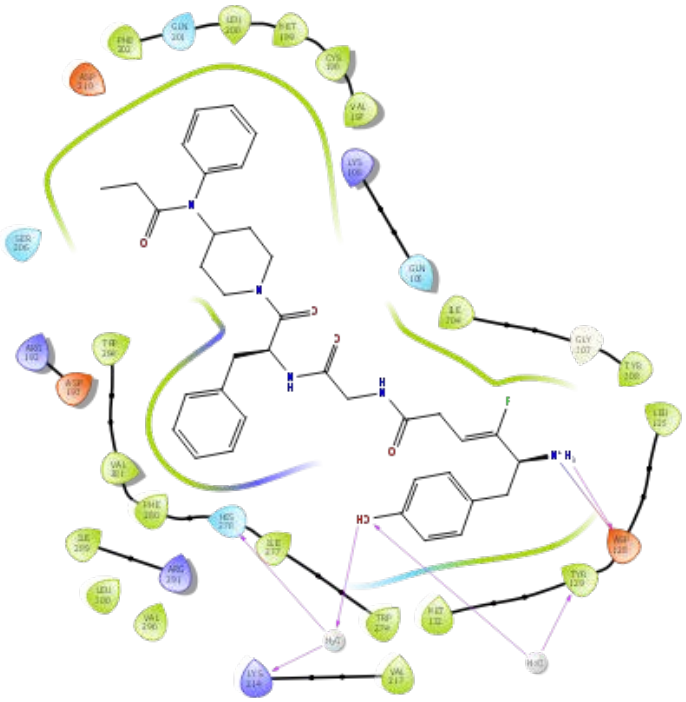

Figure SI-2: Predicted interactions between the Leu-Enkephalin analogs docked into a computation model of δOR. Analogs 1a-1f maintained the predicted π-π interaction between Phe^{4} and $W284^{(6.58)}$. Additionally, hydrogen bonding between $K108^{(2.63)}$ and $R291^{ECL3}$formed with the C-terminal of most peptides except for peptides 1b and 1c where the hydrogen bonding with $R291^{ECL3}$ was replaced by a hydrogen bonding with D193.

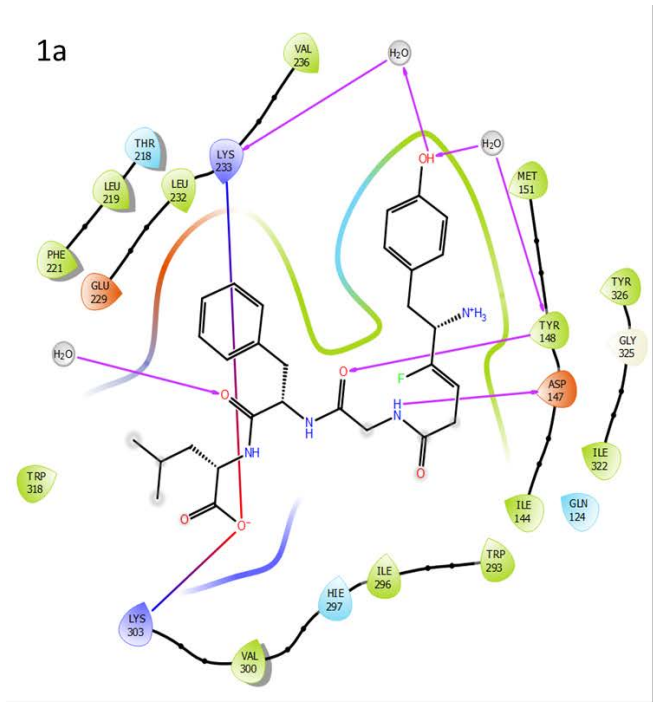
1a
VAL 236
H2O
THR 218
LYS 233
LEU 219
LEU 232
OH
H2O
MET 151
PHE 221
GLU 229
N+H3
TYR 326
TYR 148
H2O
GLY 325
O
F
ASP 147
TRP 318
NH
ILE 322
O
O-
ILE 144
GLN 124
TRP 293
ILE 296
HIE 297
LYS 303
VAL 300

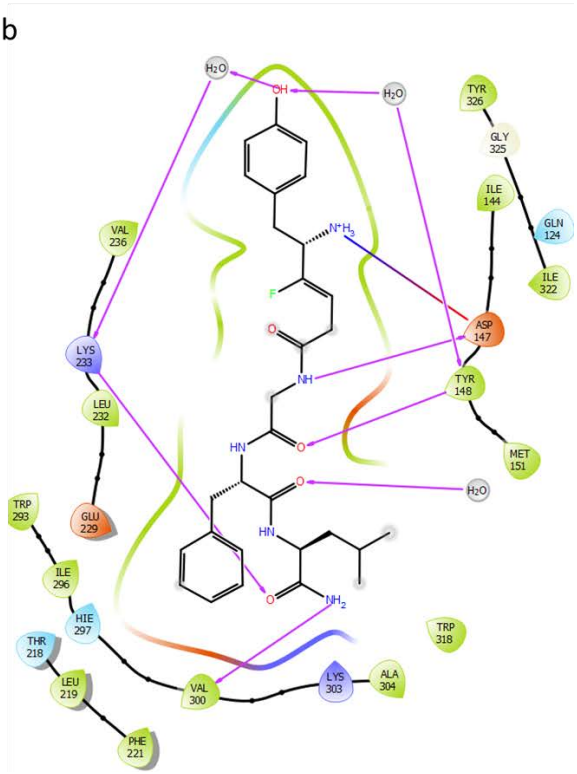
1b
H2O
OH
H2O
TYR 326
GLY 325
ILE 144
GLN 124
VAL 236
N+H3
F
ILE 322
O
ASP 147
LYS 233
NH
TYR 148
LEU 232
HN
MET 151
O
H2O
TRP 293
GLU 229
HN
ILE 296
O
NH2
HIE 297
TRP 318
THR 218
VAL 300
LYS 303
ALA 304
LEU 219
PHE 221

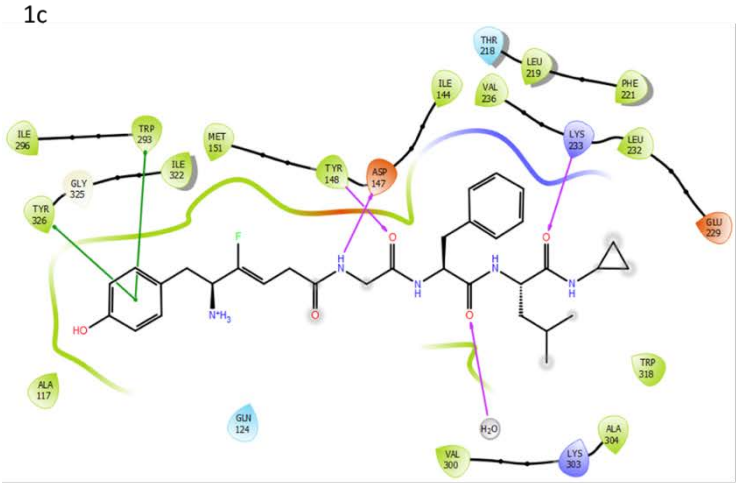
1c
THR 218
LEU 219
PHE 221
ILE 144
VAL 236
ILE 296
TRP 293
MET 151
LYS 233
LEU 232
ILE 322
GLY 325
TYR 148
ASP 147
GLU 229
TYR 326
F
O
HO
N+H3
TRP 318
ALA 117
GLN 124
H2O
VAL 300
LYS 303
ALA 304

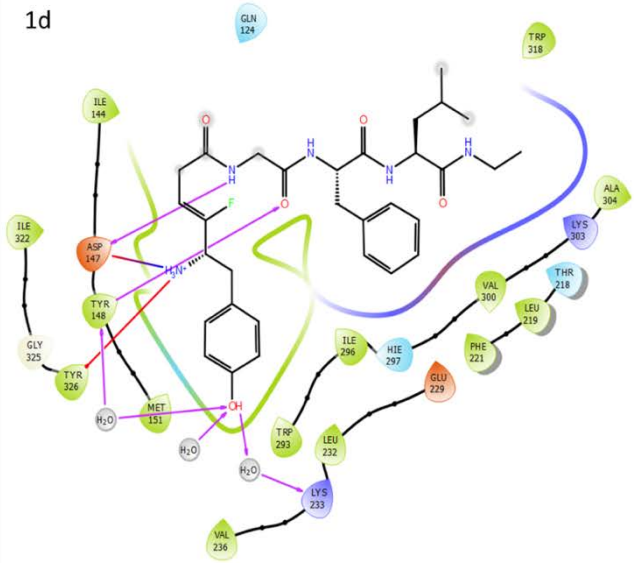
1d
GLN 124
TRP 318
ILE 144
ALA 304
ILE 322
LYS 303
ASP 147
H2N+
THR 218
VAL 300
TYR 148
LEU 219
GLY 325
ILE 296
HIE 297
PHE 221
TYR 326
GLU 229
H2O
MET 151
OH
TRP 293
LEU 232
H2O
H2O
LYS 233
VAL 236

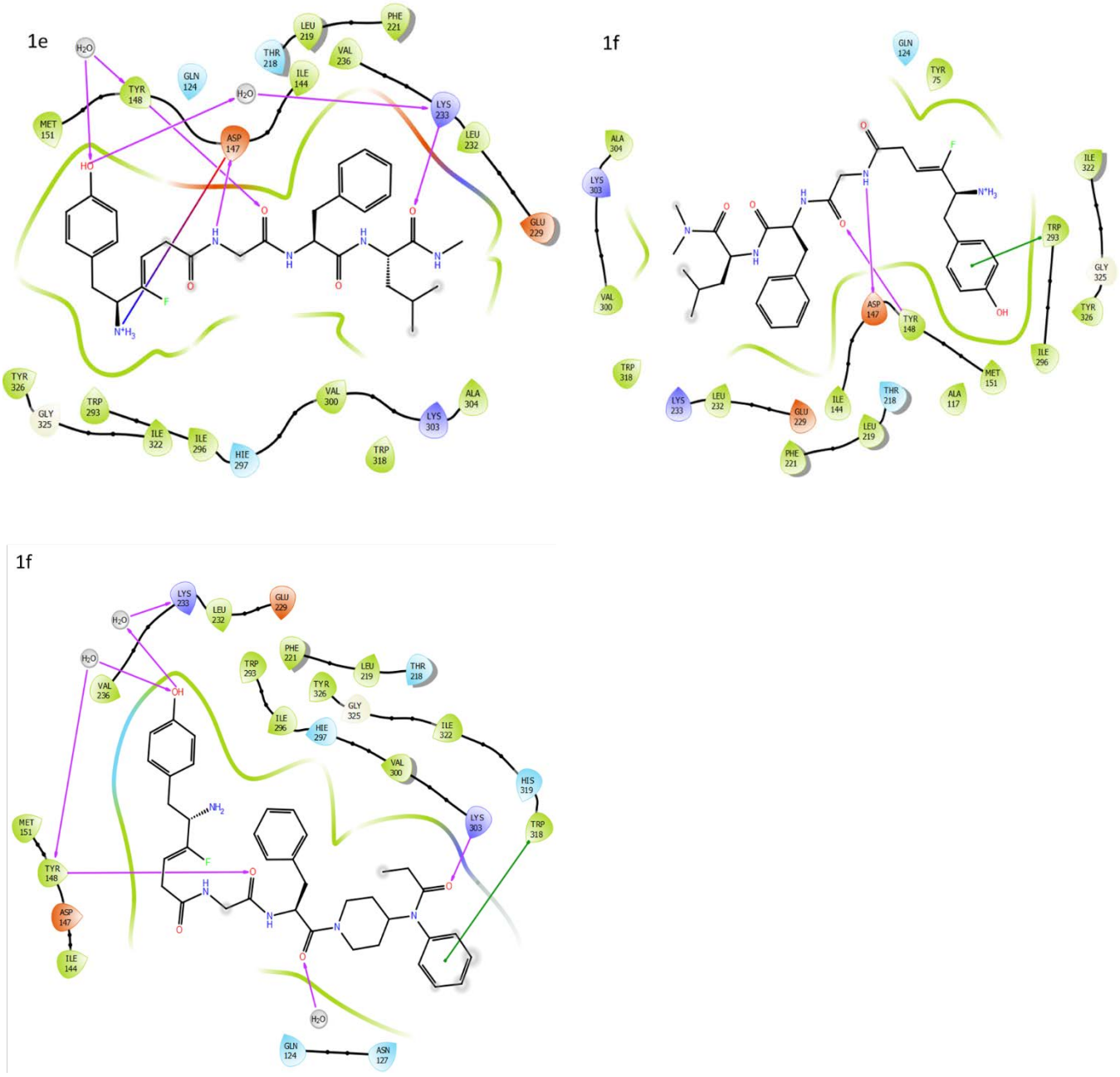

Figure SI-3: Predicted interactions between the Leu-Enkephalin analogs docked into a computational model of μOR. Most analogs 1a-1f interacted with D147$^{(3.32)}$, Y148$^{(3.33)}$, K233$^{(5.40)}$, and K303$^{(6.58)}$. However, the limited flexibility of the peptides due to the presence of the retained crystal waters in addition to the lack of a shared scaffold resulted in differences in protein-ligand interactions for each analog. Various molecular models with or without crystal waters (data not shown) failed to generate docked poses for all analogs.

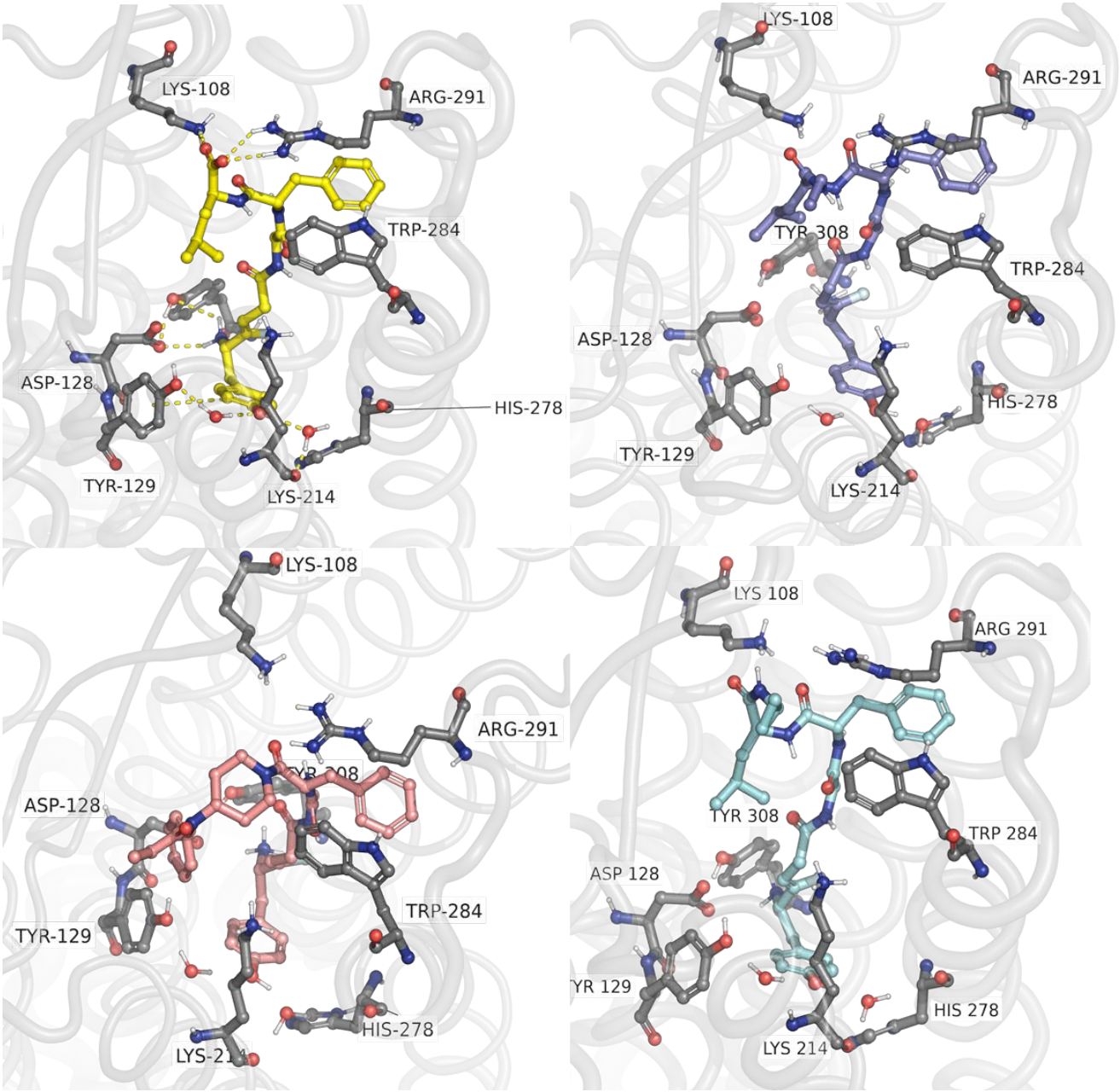

Figure SI-4: Key Interactions of Select Analogs at the δOR. The interactions between R291 and W284 are highlighted for compounds **1a** (O^-) yellow, **1d** (NHEt) purple, **1f** ($NH^{Cy}Pr$) cyan, **1g** [*N*-Pip-N(Ph)(COEt)] pink, docked into δOR.

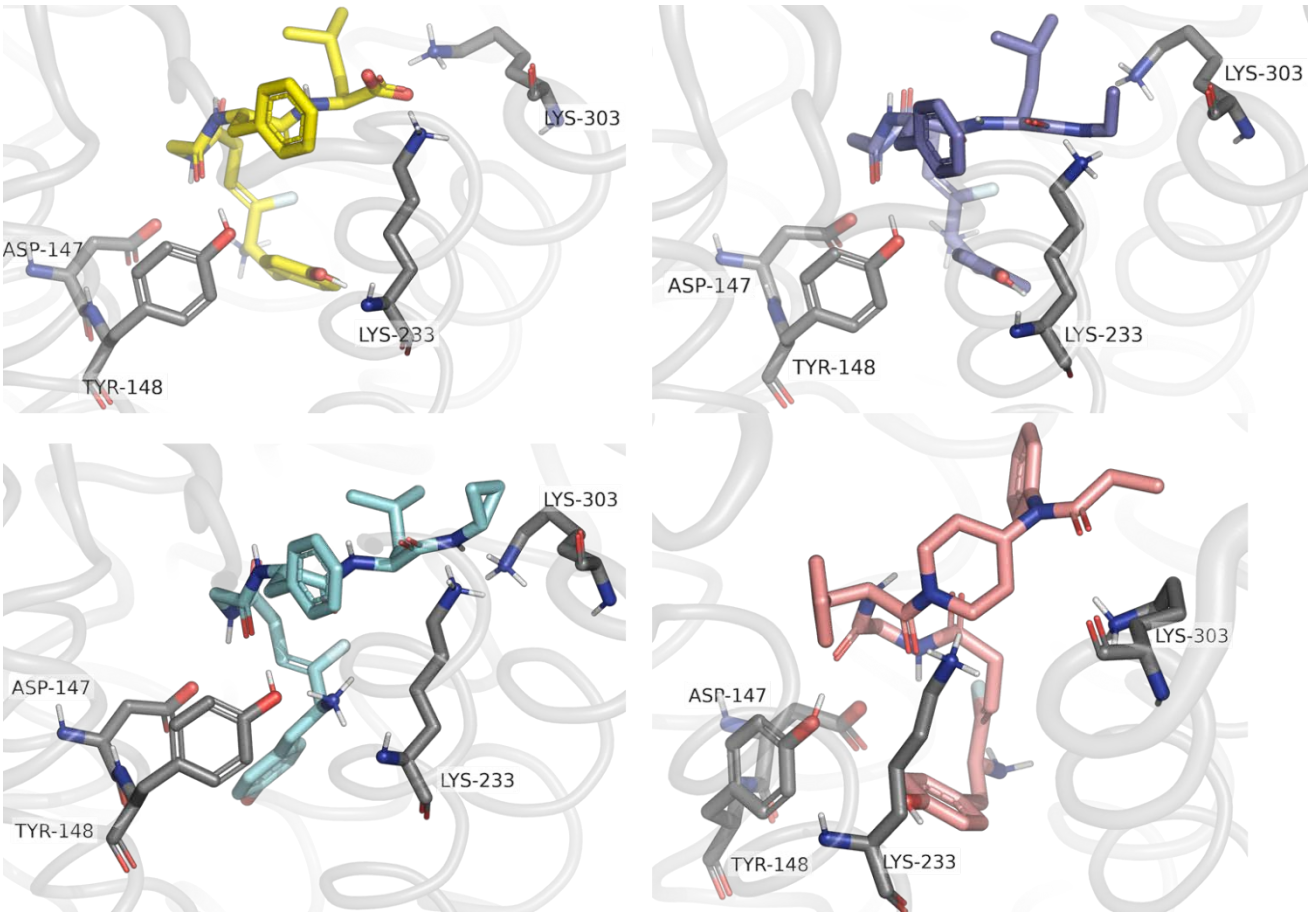

Figure SI-5: Key Interactions of Select Analogs at the μOR. The interactions between K233 and K303 are highlighted for compounds **1a** (O^-) yellow, **1d** (NHEt) purple, **1f** ($NH^{Cy}Pr$) cyan, **1g** [*N*-Pip-N(Ph)(COEt)] pink, docked into δOR.

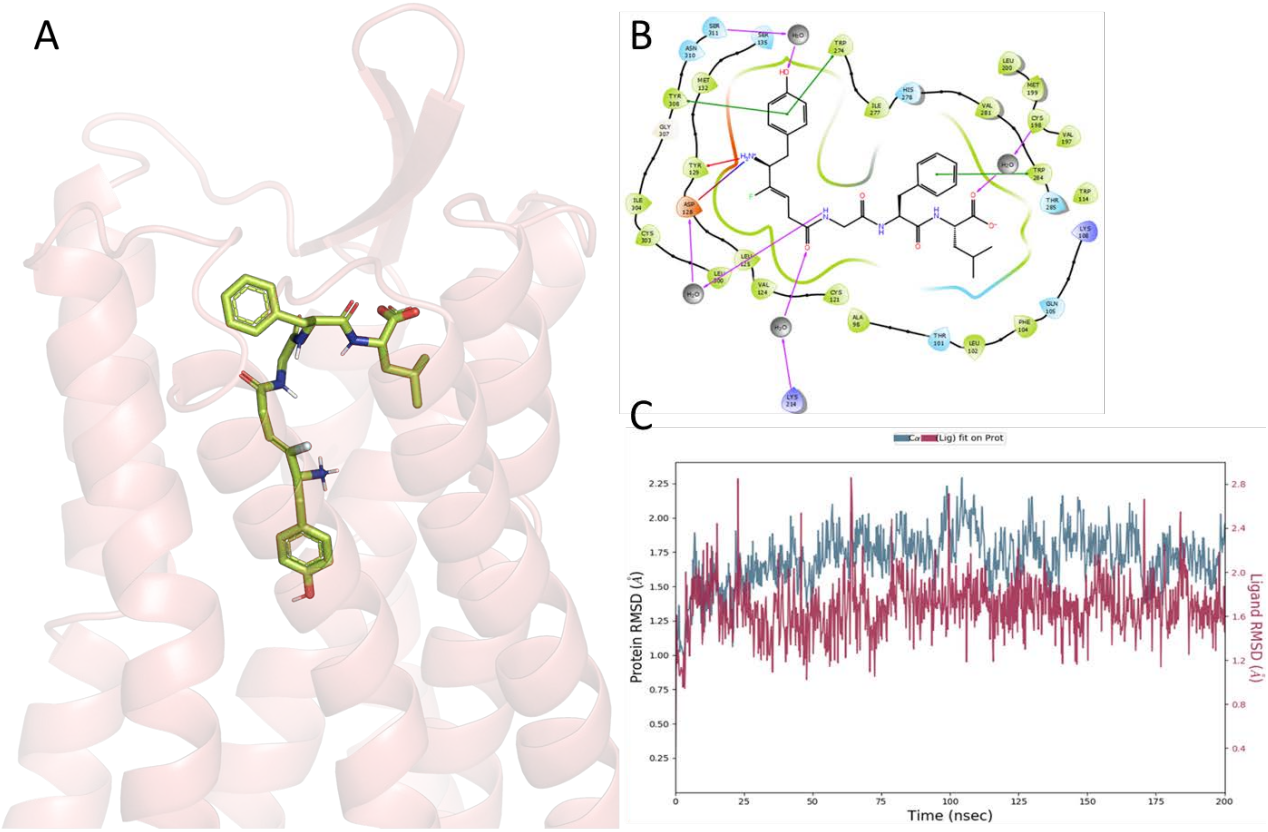

Figure SI-6: Representative figure from an all-atom 200ns MD simulation of 1a (O^-) bound to δOR. **(A)** binding pose of analog **1a** (O^-) bound to model structure of δOR where $D108^{(2.63)}$ in the crystal structure (PDB: 6PT2) was reverted to $K108^{(2.63)}$. **(B)** Peptide-receptor interactions including modeled water molecules. **(C)** Peptide and receptor RMSD over the 200ns production MD simulation**.** The 200ns MD simulation frames were clustered using the trajectory clustering utility in Schrödinger.

References

(1) Karad, S. N.; Pal, M.; Crowley, R. S.; Prisinzano, T. E.; Altman, R. A. Synthesis and Opioid Activity of Tyr 1 - ψ [(Z)CF=CH]-Gly 2 and Tyr 1 - ψ [(S)/(R)-CF 3 CH-NH]-Gly 2 Leu-Enkephalin Fluorinated Peptidomimetics. *ChemMedChem* **2017**, *12* (8), 571–576. https://doi.org/10.1002/cmdc.201700103.

(2) Mahindra, A.; Nooney, K.; Uraon, S.; Sharma, K. K.; Jain, R. Microwave-Assisted Solution Phase Peptide Synthesis in Neat Water. *RSC Adv.* **2013**, *3* (37), 16810–16816. https://doi.org/10.1039/c3ra43040e.

(3) Mahindra, A.; Sharma, K. K.; Jain, R. Rapid Microwave-Assisted Solution-Phase Peptide Synthesis. *Tetrahedron Lett.* **2012**, *53* (51), 6931–6935. https://doi.org/10.1016/j.tetlet.2012.10.028.

(4) Chiang, T.; Sansuk, K.; van Rijn, R. M. β-Arrestin 2 Dependence of δ Opioid Receptor Agonists Is Correlated with Alcohol Intake. *Br. J. Pharmacol.* **2016**, *173* (2), 332–343. https://doi.org/10.1111/bph.13374.

(5) Altman, R. A.; Sharma, K. K.; Rajewski, L. G.; Toren, P. C.; Baltezor, M. J.; Pal, M.; Karad, S. N. Tyr1-ψ[(Z)CF=CH]-Gly2 Fluorinated Peptidomimetic Improves Distribution and Metabolism Properties of Leu-Enkephalin. *ACS Chem. Neurosci.* **2018**, *9* (7), 1735–1742. https://doi.org/10.1021/acschemneuro.8b00085.

(6) Weinberger, S. B.; Martinez, J. L. J. Characterization of Hydrolysis of [Leu] Enkephalin in Rat Plasma. *J. Pharmacol. Exp. Ther* . **1988**, *247*, 129–135.

(7) Roques, B. P.; Noble, F. Dual Inhibitors of Enkephalin-Degrading Enzymes (Neutral Endopeptidase 24.11 and Aminopeptidase N) as Potential New Medications in the Management of Pain and Opioid Addiction. *NIDA Res. Monogr.* **1995**, *147* (147), 104–145.

(8) Thompson, S. E.; Audus, K. L. Leucine-Enkephalin Metabolism in Brain Microvessel Endothelial Cells. *Peptides* **1994**, *15* (1), 109–116. https://doi.org/10.1016/0196-9781(94)90178-3.

(9) Claff, T.; Yu, J.; Blais, V.; Patel, N.; Martin, C.; Wu, L.; Han, G. W.; Holleran, B. J.; Van der Poorten, O.; White, K. L.; Hanson, M. A.; Sarret, P.; Gendron, L.; Cherezov, V.; Katritch, V.; Ballet, S.; Liu, Z. J.; Müller, C. E.; Stevens, R. C. Elucidating the Active δ-Opioid Receptor Crystal Structure with Peptide and Small-Molecule Agonists. *Sci. Adv.* **2019**, *5* (11), eaax9115. https://doi.org/10.1126/sciadv.aax9115.

(10) Huang, W.; Manglik, A.; Venkatakrishnan, A. J.; Laeremans, T.; Feinberg, E. N.; Sanborn, A. L.; Kato, H. E.; Livingston, K. E.; Thorsen, T. S.; Kling, R. C.; Granier, S.; Gmeiner, P.; Husbands, S. M.; Traynor, J. R.; Weis, W. I.; Steyaert, J.; Dror, R. O.; Kobilka, B. K. Structural Insights into M-Opioid Receptor Activation. *Nature* **2015**, *524* (7565), 315–321. https://doi.org/10.1038/nature14886.

(11) Prime. In Schrödinger Release 2021-1. Schrödinger, LLC: New York, NY 2021.

(12) Jacobson, M. P.; Friesner, R. A.; Xiang, Z.; Honig, B. On the Role of the Crystal Environment in Determining Protein Side-Chain Conformations. *J. Mol. Biol.* **2002**, *320* (3), 597–608. https://doi.org/10.1016/S0022-2836(02)00470-9.

(13) Jacobson, M. P.; Pincus, D. L.; Rapp, C. S.; Day, T. J. F.; Honig, B.; Shaw, D. E.; Friesner, R. A. A Hierarchical Approach to All-Atom Protein Loop Prediction. *Proteins Struct. Funct. Bioinforma.* **2004**, *55* (2), 351–367. https://doi.org/10.1002/prot.10613.

(14) Harder, E.; Damm, W.; Maple, J.; Wu, C.; Reboul, M.; Xiang, J. Y.; Wang, L.; Lupyan, D.; Dahlgren, M. K.; Knight, J. L.; Kaus, J. W.; Cerutti, D. S.; Krilov, G.; Jorgensen, W. L.; Abel, R.; Friesner, R. A. OPLS3: A Force Field Providing Broad Coverage of Drug-like Small Molecules and Proteins. *J. Chem. Theory Comput.* **2016**, *12* (1), 281–296. https://doi.org/10.1021/acs.jctc.5b00864.

(15) Shivakumar, D.; Williams, J.; Wu, Y.; Damm, W.; Shelley, J.; Sherman, W. Prediction of Absolute Solvation Free Energies Using Molecular Dynamics Free Energy Perturbation and the Opls Force Field. *J. Chem. Theory Comput.* **2010**, *6* (5), 1509–1519. https://doi.org/10.1021/ct900587b.

(16) Jorgensen, W. L.; Maxwell, D. S.; Tirado-Rives, J. Development and Testing of the OPLS All-Atom Force Field on Conformational Energetics and Properties of Organic Liquids. *J. Am. Chem. Soc.* **1996**, *118* (45), 11225–11236. https://doi.org/10.1021/ja9621760.

(17) Greenwood, J. R.; Calkins, D.; Sullivan, A. P.; Shelley, J. C. Towards the Comprehensive, Rapid, and Accurate Prediction of the Favorable Tautomeric States of Drug-like Molecules in Aqueous Solution. *J. Comput. Aided. Mol. Des.* **2010**, *24* (6–7), 591–604. https://doi.org/10.1007/s10822-010-9349-1.

(18) Shelley, J. C.; Cholleti, A.; Frye, L. L.; Greenwood, J. R.; Timlin, M. R.; Uchimaya, M. Epik: A Software Program for PK a Prediction and Protonation State Generation for Drug-like Molecules. *J. Comput. Aided. Mol. Des.* **2007**, *21* (12), 681–691. https://doi.org/10.1007/s10822-007-9133-z.

(19) Friesner, R. A.; Banks, J. L.; Murphy, R. B.; Halgren, T. A.; Klicic, J. J.; Mainz, D. T.; Repasky, M. P.; Knoll, E. H.; Shelley, M.; Perry, J. K.; Shaw, D. E.; Francis, P.; Shenkin, P. S. Glide: A New Approach for Rapid, Accurate Docking and Scoring. 1. Method and Assessment of Docking Accuracy. *J. Med. Chem.* **2004**, *47* (7), 1739–1749. https://doi.org/10.1021/jm0306430.

(20) Halgren, T. A.; Murphy, R. B.; Friesner, R. A.; Beard, H. S.; Frye, L. L.; Pollard, W. T.; Banks, J. L. Glide: A New Approach for Rapid, Accurate Docking and Scoring. 2. Enrichment Factors in Database Screening. *J. Med. Chem.* **2004**, *47* (7), 1750–1759. https://doi.org/10.1021/jm030644s.

(21) Schrödinger Release 2019-4: Protein Preparation Wizard; Epik; Impact; Prime; Glide; LigPrep; Induced Fit Docking Protocol: New York, NY.

(22) Cassell, R. J.; Sharma, K. K.; Su, H.; Cummins, B. R.; Cui, H.; Mores, K. L.; Blaine, A. T.; Altman, R. A.; van Rijn, R. M. The Meta-Position of Phe4 in Leu-Enkephalin Regulates Potency, Selectivity, Functional Activity, and Signaling Bias at the Delta and Mu Opioid Receptors. *Molecules* **2019**, *24* (24), 4542. https://doi.org/10.3390/molecules24244542.

(23) Desmond Molecular Dynamics System and Maestro-Desmond Interoperability Tools. In Schrödinger Release 2021-1; Schrödinger, LLC: New York, NY.

(24) Madhavi Sastry, G.; Adzhigirey, M.; Day, T.; Annabhimoju, R.; Sherman, W. Protein and Ligand Preparation: Parameters, Protocols, and Influence on Virtual Screening Enrichments. *J. Comput. Aided. Mol. Des.* **2013**, *27* (3), 221–234. https://doi.org/10.1007/s10822-013-9644-8.